Stellar Intensity Interferometry with NectarCAM on the MSTs-N

with numerous inputs from LST and MST colleagues
incl. particularly significant inputs from **Tarek Hassan** *(LST team, CIEMAT)*

2024.09.13

J. Biteau & Q. Luce, IJCLab / Univ. Paris Sa

ɣ-ray game changer: Cherenkov Telescope Array Observatory

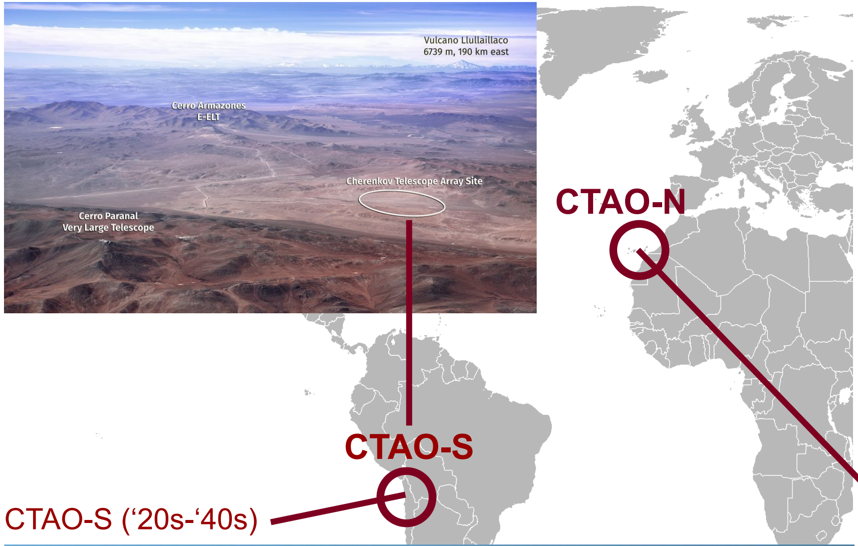

HEGRA (‘90s)

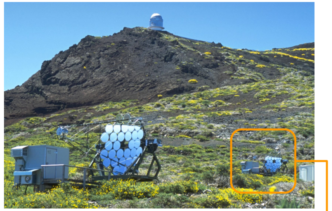

2 sites to access the entire sky w/ breakthrough performance

Sensitivity: 5-10× better than current

E-range: 0.02-200 TeV (vs 0.1-10 TeV)

E-resolution: <10% (vs <17%) >0.2 TeV

MAGIC (‘00s,’10s)

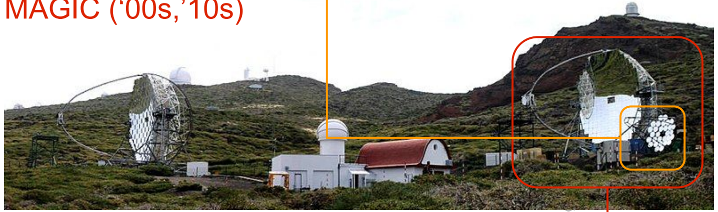

CTAO-S (‘20s-‘40s)

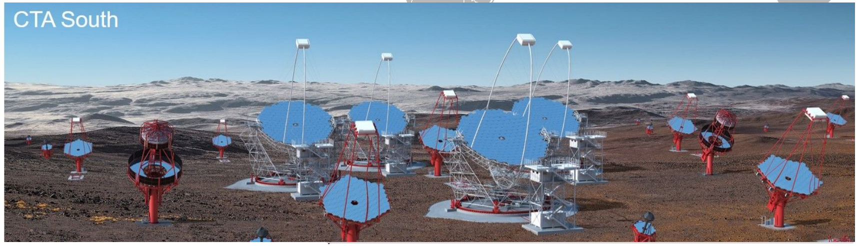

CTAO-N (‘20s-‘40s)

Credit: Gabriel Pérez Díaz, I

The MSTs on the CTAO-North Site

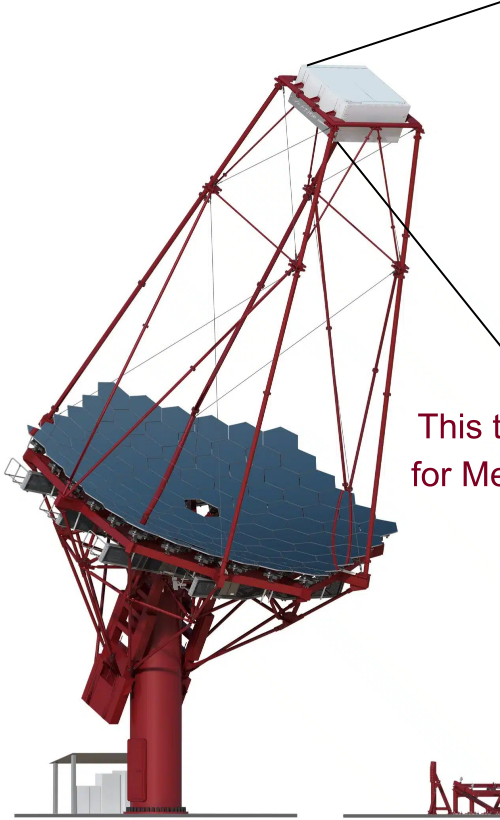

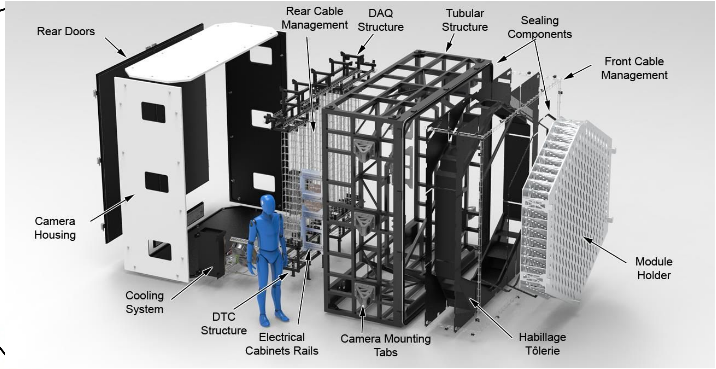

Credits: O. Ferreira

This talk by Jonathan Biteau & Quentin Luce (IJCLab) for Medium Sized Telescopes (MSTs) with NectarCAMs

see talk by Juan Cortina & Alejo Cifuentes (CIEMAT) for Large Sized Telescopes (LSTs) on Wed.

Credit: Gabriel Pérez Diaz,

The MSTs on the CTAO-North Site

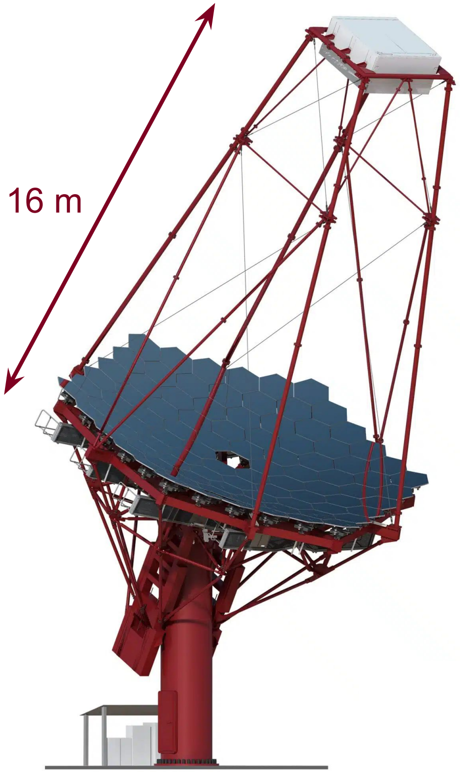

NectarCAM

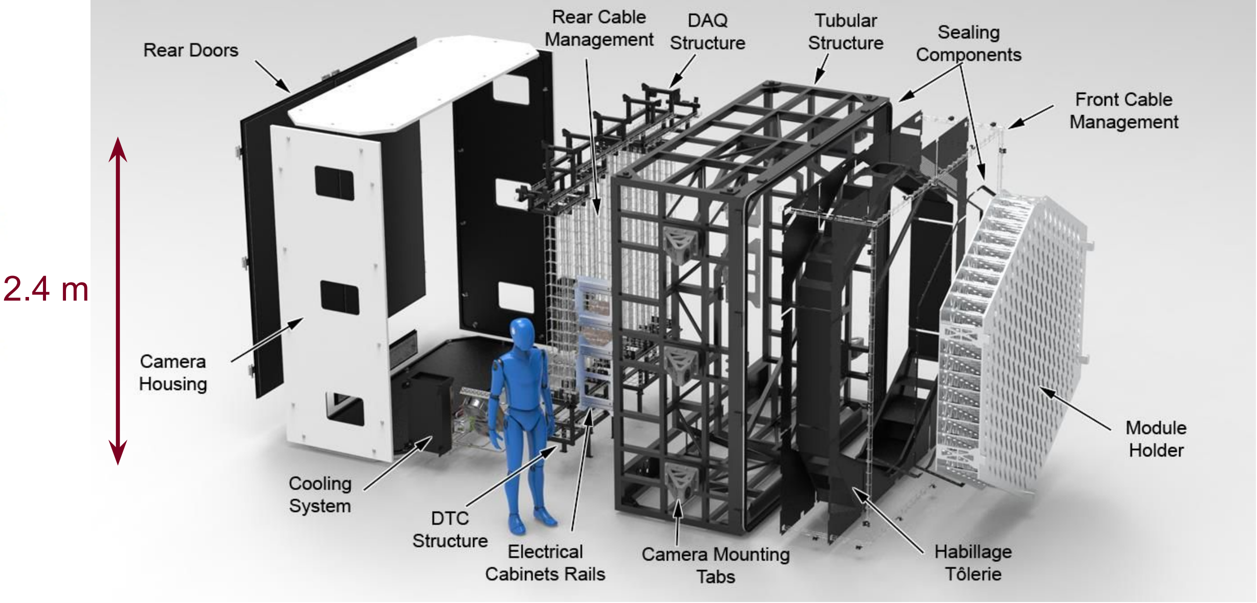

Detection modules of NectarCAM

Credits: A. Tsihahina & O. Ferreira

265 ×

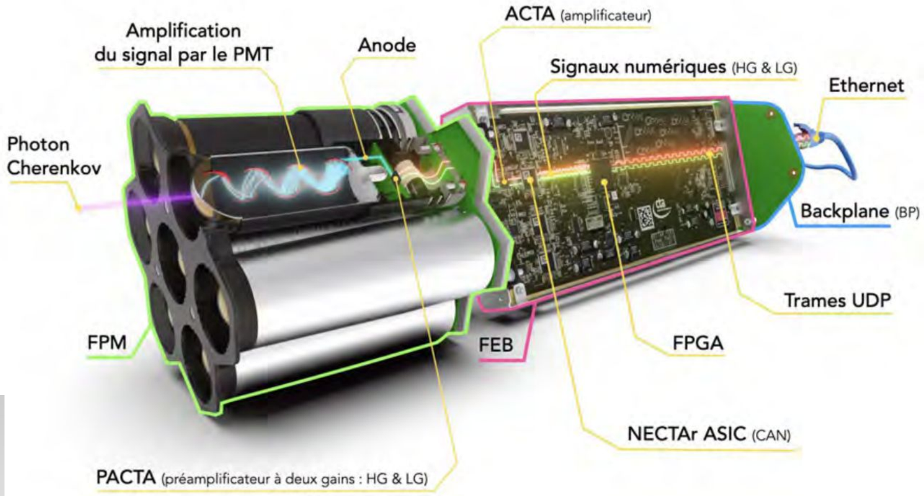

= 1855 photo-multiplier tubes, with a field of view of 0.18° each, for a total field of view of 8°

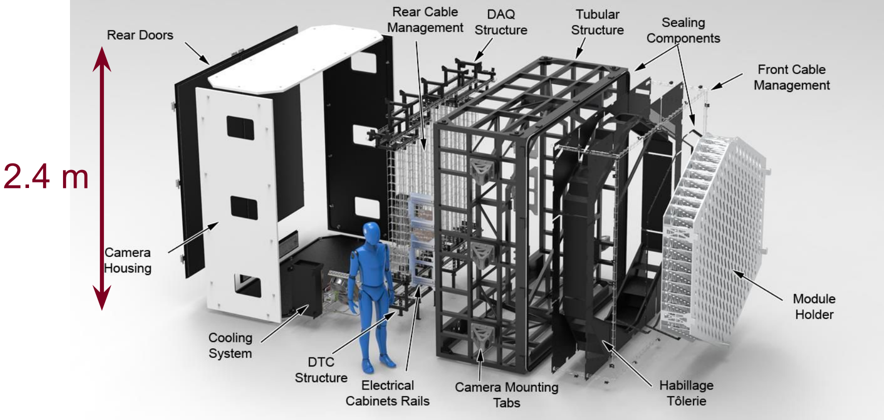

In the field?

Credits: DESY

Credits: IRFU CEA/Saclay

In the field?

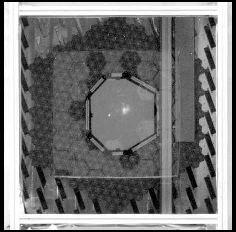
Star image
⇓
Mirror alignment
⇓
Angular resolution

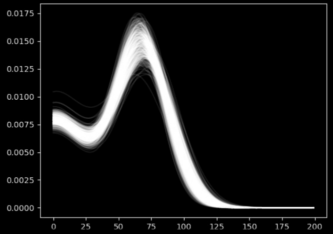

SPE response
⇓
Gain of each channel
⇓
Energy resolution

Calibration devices of NectarCAM

Critical design & manufacturing review ☑
→ in production for 9 cameras + spares

Thanks to great IJCLab R&D team,
as well as Barbara Biasuzzi's postdoc,
Pooja Sharma's thesis, Sonal Patel's postdoc,
Coline Dubos's thesis

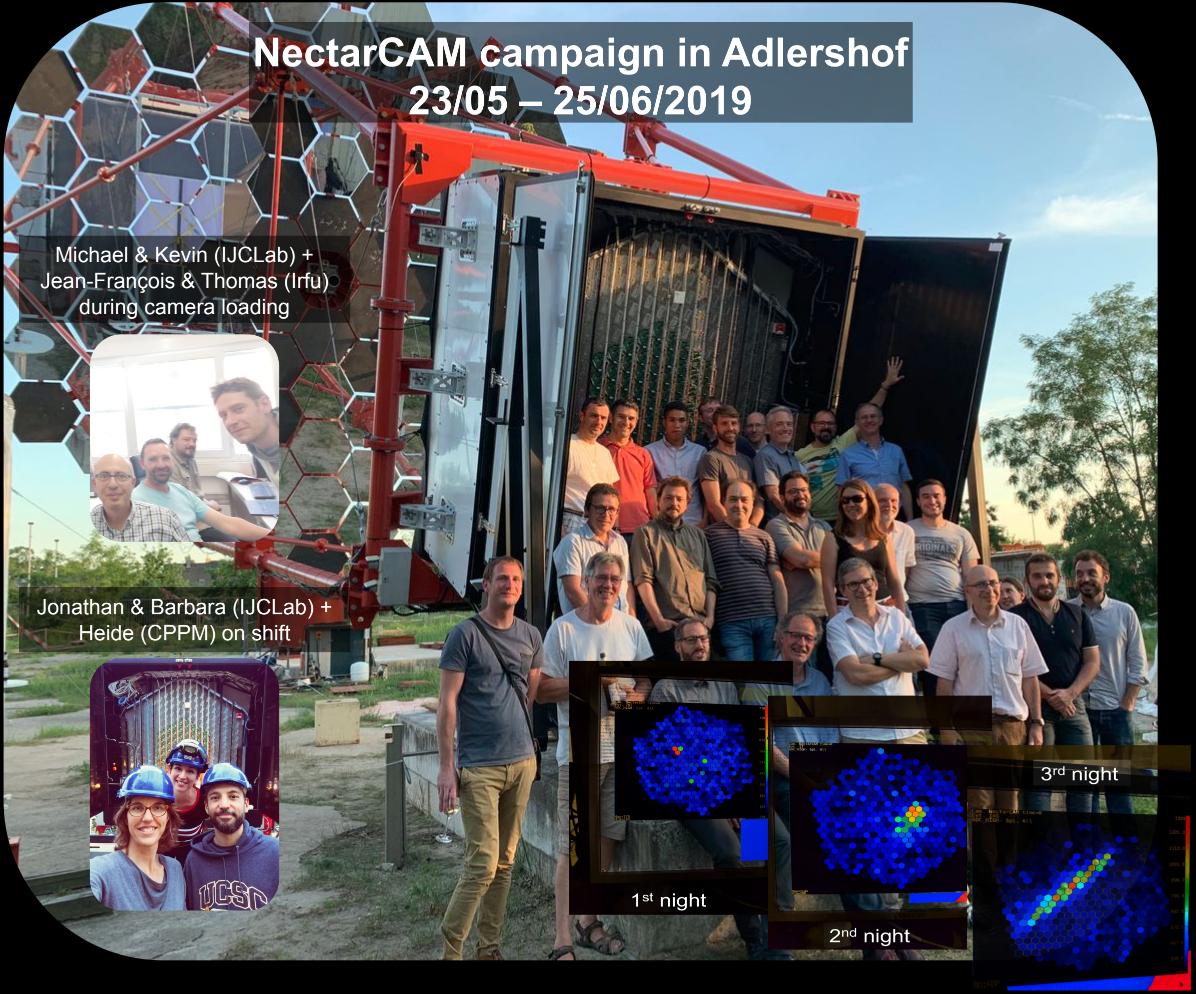

NectarCAM campaign in Adlershof
23/05 – 25/06/2019

Michael & Kevin (IJCLab) +
Jean-François & Thomas (Irfu)
during camera loading

Jonathan & Barbara (IJCLab) +
Heide (CPPM) on shift

From 2020 to 2023

Part 1 - MST/NectarCAM implementation

Triggered by a talk by **Tarek Hassan**
at the Nov. 2022 CTAO Consortium meeting in Napoli

SII with medium-sized telescopes (MSTs) at CTAO-North?

Including MSTs in the SII array improves:

- Extent of the coverage of spatial frequencies (*uv*-plane) → Order-of-magnitude improved precision on ~100 μas stellar radius
- Density of uv coverage: **never achieved so far**! → True capacity for “model-based” imaging (phase is unknown)

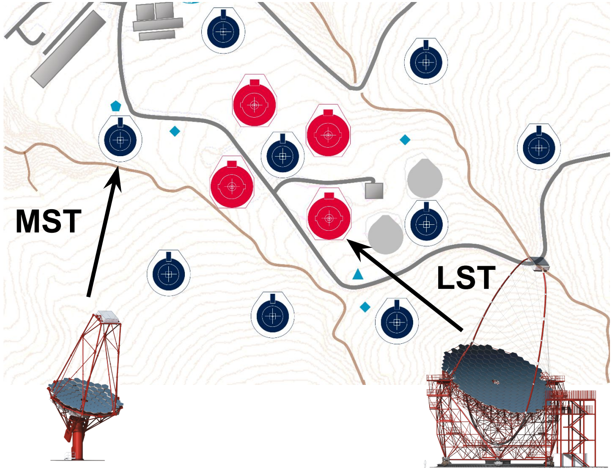

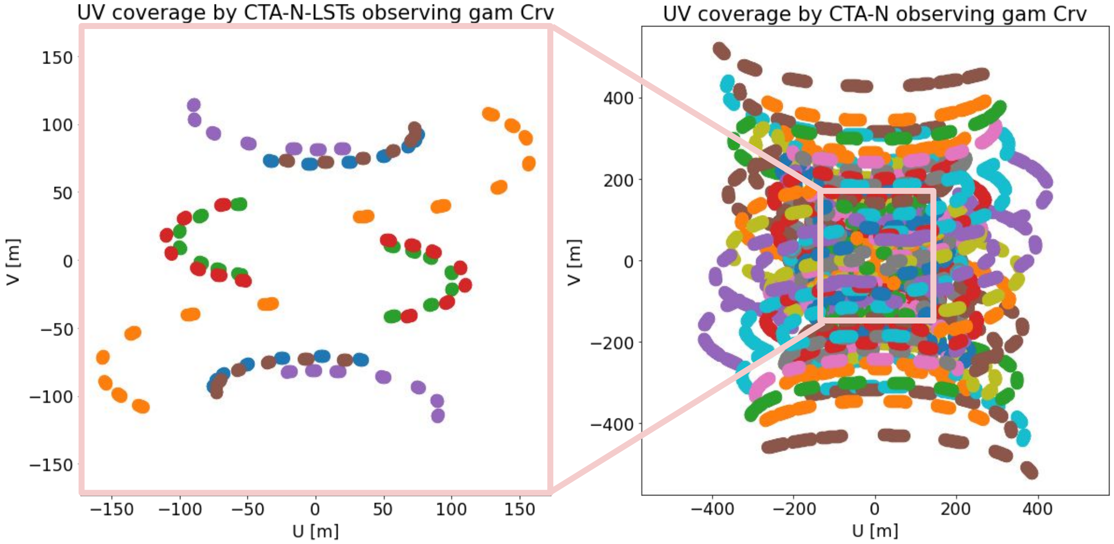

Credits: **Tarek Hassan**

Modifications of the camera

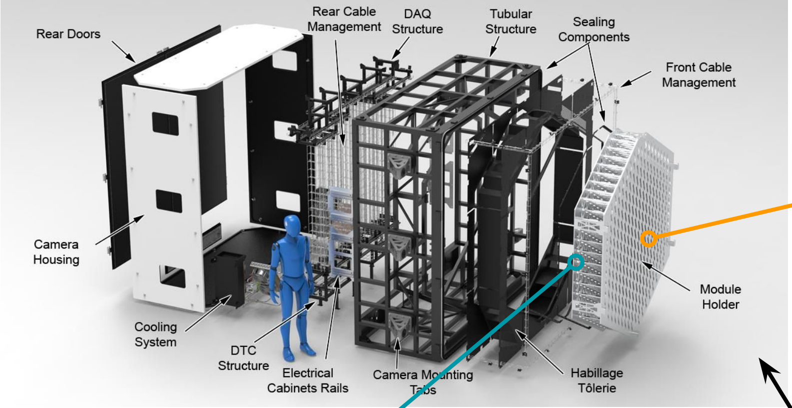

Movable filters
(two sets of ON/OFF)

Credits for NectarCAM
Kevin Pressard (IJCLab)

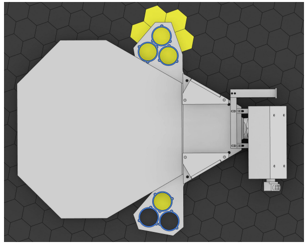

Amplification of anode current and optical transmission

Credits for LST1
Gustavo Martínez
(CIEMAT)

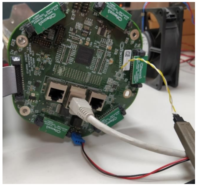

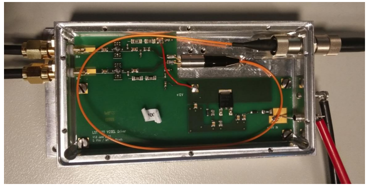

Credits for LST1
David Fink
(MPI Phys)

NectarCAM 1

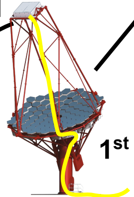

1st MST

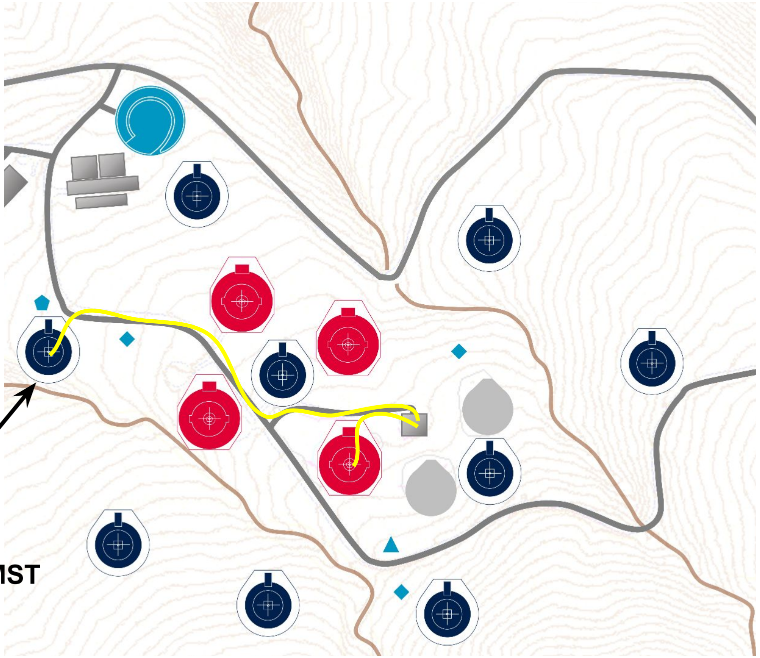

Filters for NectarCAM

Same concept as in LST-1 and MAGIC

MST/NectarCAM camera

Credits for NectarCAM
Kevin Pressard (IJCLab)

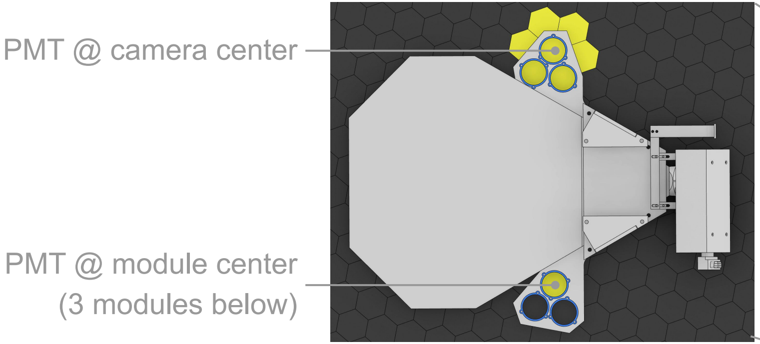

Movable filters

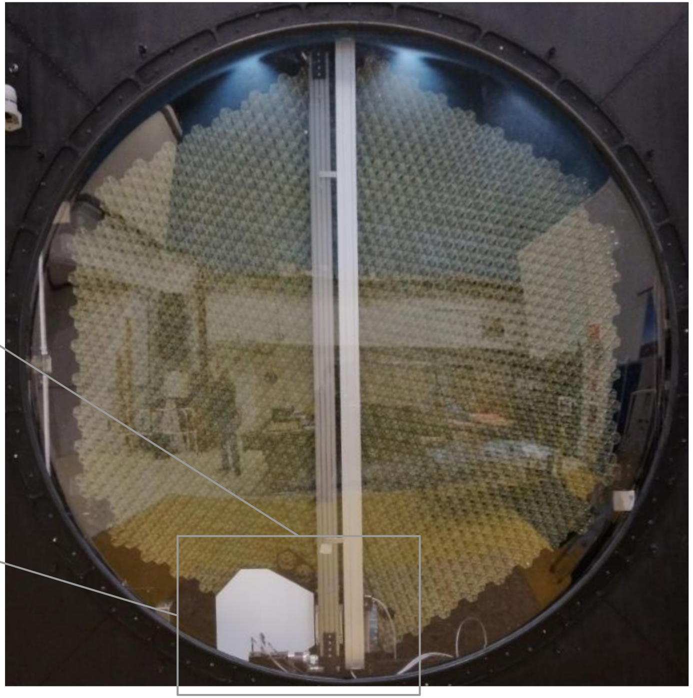

Semrock filters 425/26 nm, with ∅ = 40 mm for NectarCAM

Filters for NectarCAM

Same concept as in LST-1 and MAGIC

MST/NectarCAM camera

Credits for NectarCAM
Kevin Pressard (IJCLab)

PMT @ camera center

PMT @ module center
(3 modules below)

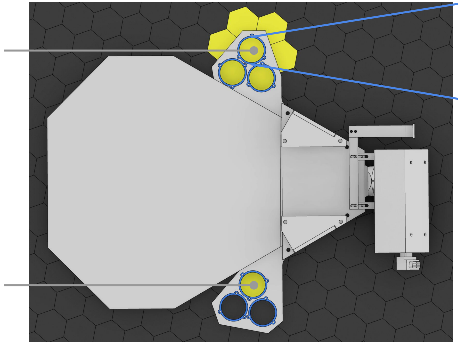

Movable filters

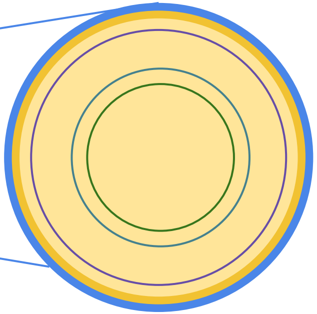

⌀**(filter)** = 40 mm
⌀**(filter-mount)** = 38 mm
⌀**(usable area)** = 36 mm
$\varnothing_{\mathrm{PSF}}$**(95, 80, 68 %)** = 33, 23, 19 mm

Semrock filters 425/26 nm, with ⌀ = 40 mm for NectarCAM

Note: pointing accuracy of 7” ↔ 0.5mm at a focal length of 16m

Filters for NectarCAM

Same concept as in LST-1 and MAGIC

MST/NectarCAM camera

Credits for NectarCAM
Kevin Pressard (IJCLab)

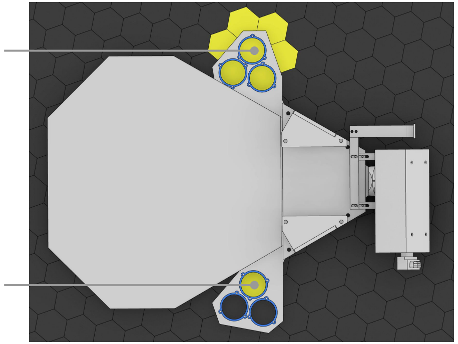

PMT @ camera center

PMT @ module center
(3 modules below)

Movable filters

1 ON + 5 OFF

At this stage, 1 PMT (central) + **5 OFF regions**
→ goal: increase precision on night-sky background

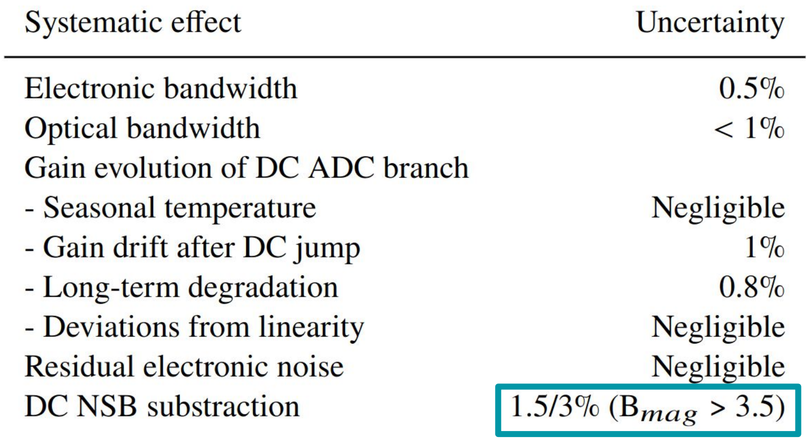

Systematic effect	Uncertainty
Electronic bandwidth	0.5%
Optical bandwidth	< 1%
Gain evolution of DC ADC branch	
- Seasonal temperature	Negligible
- Gain drift after DC jump	1%
- Long-term degradation	0.8%
- Deviations from linearity	Negligible
Residual electronic noise	Negligible
DC NSB substraction	1.5/3% ($B_{mag} > 3.5$)

Table 5. Evaluated systematic uncertainties over squared visibility measurements identified to effect the MAGIC-SII system.

Credits: MAGIC SII paper

Semrock filters 425/26 nm, with ⌀ = 40 mm for NectarCAM

Note: pointing accuracy of 7” ↔ 0.5mm at a focal length of 16m

Filters for NectarCAM

Same concept as in LST-1 and MAGIC

At this stage, 1 PMT (central) + **5 OFF regions**

or 1 PMT (central) + **2 OFF** ➕ **1 PMT** (off-axis) + **2 OFF**

MST/NectarCAM camera

Credits for NectarCAM
Kevin Pressard (IJCLab)

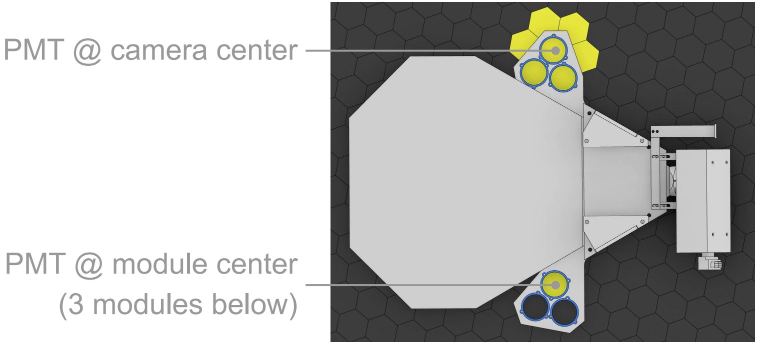

Movable filters

1 ON + 5 OFF
or 2 × (1 ON + 2 OFF)

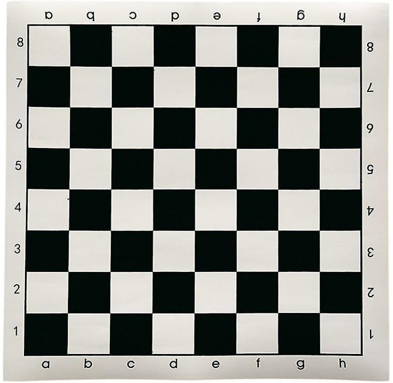

chessboard

Semrock filters 425/26 nm, with ⌀ = 40 mm for NectarCAM

Note: pointing accuracy of 7” ↔ 0.5mm at a focal length of 16m

Filters for NectarCAM

Same concept as in LST-1 and MAGIC

MST/NectarCAM camera

Credits for NectarCAM
Kevin Pressard (IJCLab)

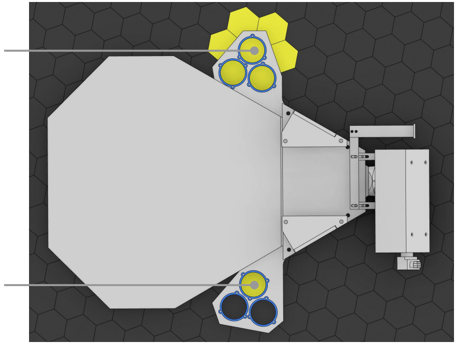

PMT @ camera center

PMT @ module center
(3 modules below)

Movable filters

1 ON + 5 OFF
or 2 × (1 ON + 2 OFF)

Semrock filters 425/26 nm, with ∅ = 40 mm for NectarCAM

Note: pointing accuracy of 7" ↔ 0.5mm at a focal length of 16m

At this stage, 1 PMT (central) + **5 OFF regions**

or 1 PMT (central) + **2 OFF** ➕ **1 PMT** (off-axis) + **2 OFF**

or 1 PMT + 2 OFF @ 420nm

➕ **1 PMT + 2 OFF @ <u>emission line</u>**

Credits; JWST

Retrieving the signal

Production of 18 upgraded backplanes

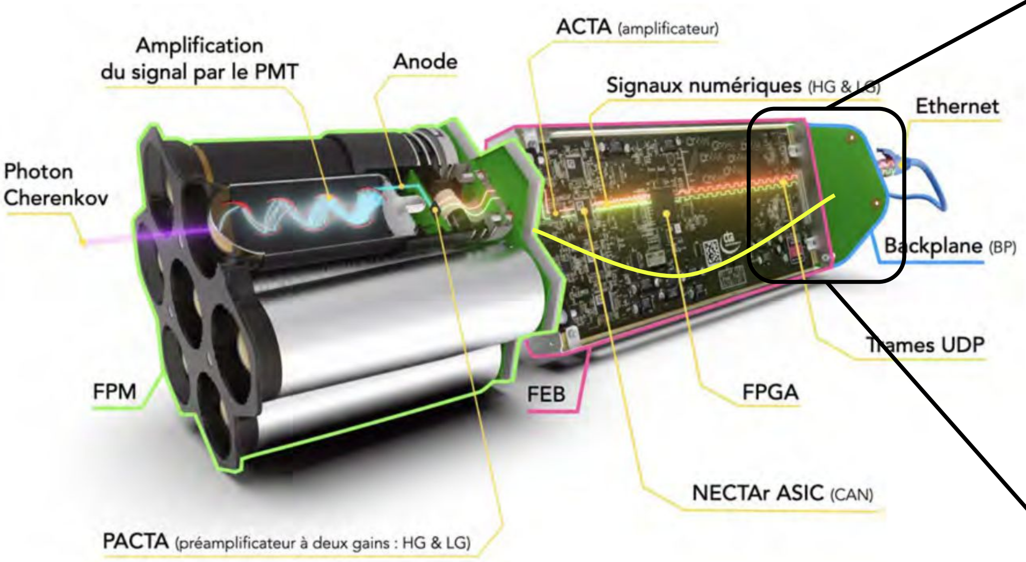

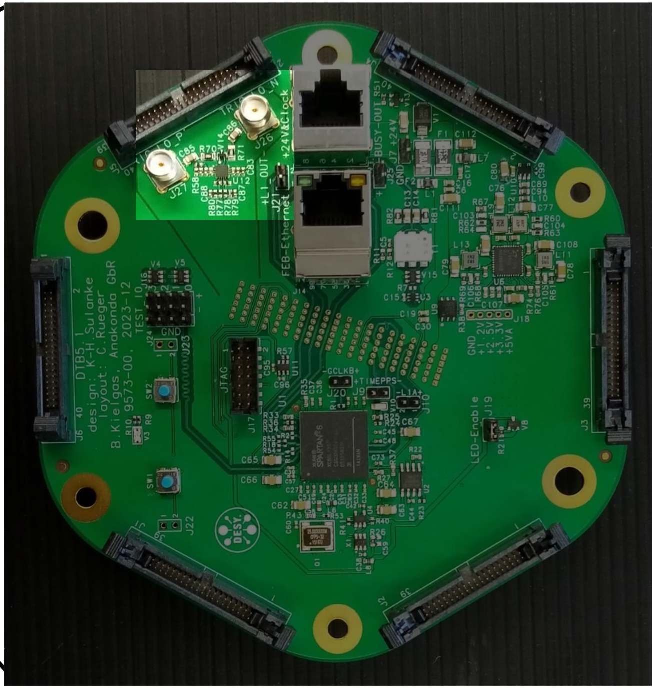

Credits: Karl-Heinz Sulanke (DESY)

Retrieving the signal

Limitations for electronic bandwidth

→ Transit time (“jitter”) of photomultiplier tubes:

1.5 ns (rms)

→ Shape of the dish:

LST: -

MST: 0.7 ns (rms)

Goal: 500 MHz bandwidth

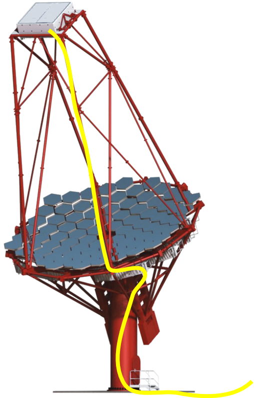

CTA-N	Large-Sized Telescope (LST)	Medium-Sized Telescope (MST)
	Mechanics	
Number of telescopes	4	9
Effective mirror area (including **shadowing**)	370 m²	88 m²
Primary reflector diameter	23 m	11.5 m
Focal length	28 m	16 m
Optical design	Parabolic	Modified Davies-Cotton
Arrival time standard deviation	-	0.7 ns
Pixel size (imaging)	6 arcmin	10 arcmin
	Optics	
Cone half angle	22 deg	20 deg
Optical efficiency at 420 nm, incl. mirror reflectivity, ~~shadowing~~, entrance window, filters, light cones	0.64	0.73
Normalized spectral distribution with a 420 nm filter, for a 21 deg cone	0.91	
	Photodetection	
PMT excess noise factor	1.21	
PMT quantum efficiency at 420 nm	39%	
PMT transit time standard deviation at 1 p.e.	1.5 ns	
	Bandwidth	
Maximum electronic bandwidth	650 MHz	600 MHz

Transmission of the signal

Option 1: VCSEL-based system (MPI Phys.) as in LST & MAGIC

Amplification of anode current and optical transmission

Credits for LST1 Gustavo Martinez (CIEMAT)

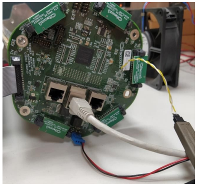

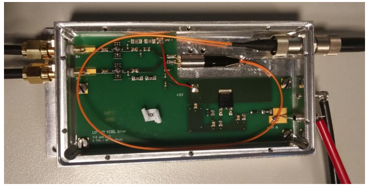

Credits for LST1 David Fink (MPI Phys)

sent through 50/125µm multi-mode fiber @ λ = 850 nm

Credits: MAGIC SII paper

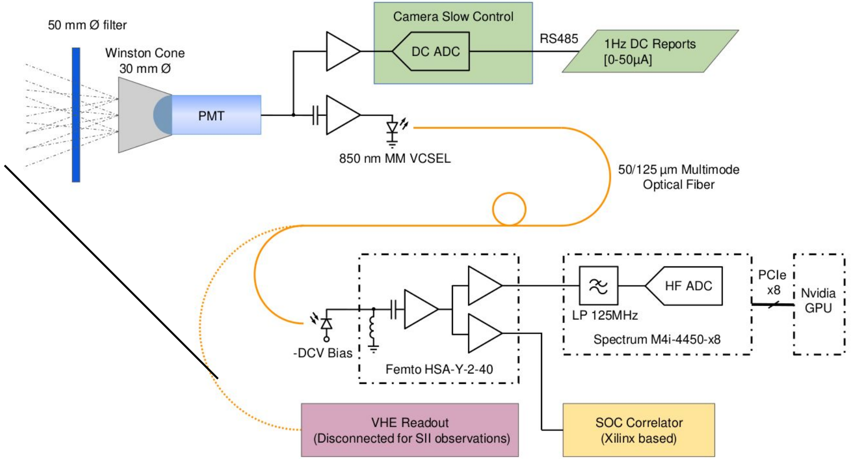

Option 2: Off-the-shelf (equivalent?) as in VERITAS

Electrical — **Optical** — **Electrical** — **Digital** — **FFT** →

sent through 10µm single-mode fiber @ λ = 1550 nm

Transmission of the signal

Option 3: IDROGEN board (IJCLab) developed for radio astronomy

PAON4, experiment @ Nancay - Credits: Ansari+ 2019

Now: 2 channels with 0.5 GS/s @ 14 bits

Electrical → **Digital** → **FFT** →

Upcoming: 1 channel with 1 GS/s

Credits: MAGIC SII paper

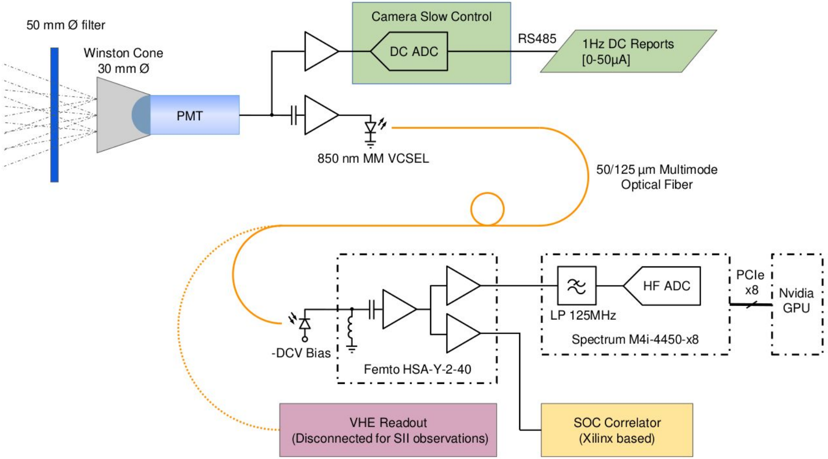

Electrical → **Optical** → **Electrical** → **Digital** → **FFT** →

Summary & next steps for NectarCAM

Routing of the signal *Julie Prast (LAPP), Alex Steiner (DESY), Oscar Ferreira (LLR)*

- from camera to telescope pedestal ✓

Definition and mounting of filters *Kevin Pressard (IJCLab)*

- full compatibility with filters chosen for LST ✓

Anode signal → Optical fiber *Kale Sulanke (DESY), François Toussenel (LPNHE), David Fink (MPP), Eric Delagne (IRFU, CEA/Saclay)*

- signal conditioning ✓
- signal degradation about to be measured

NectarCAM operation

- sampling at ~Hz rate of ON/OFF pixel current
- definition of the observing mode

Prepare SII observations with NectarCAM

- end-to-end validation of signal transmission
- characterize NectarCAM performance for SII in Irfu dark room
- explore the science case to prepare 1st observations

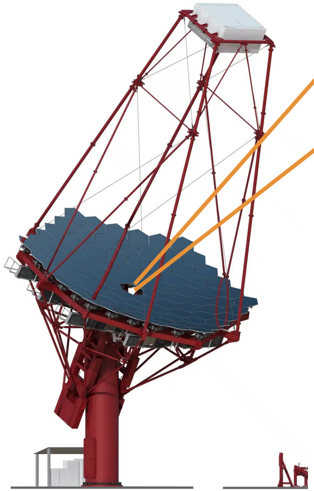

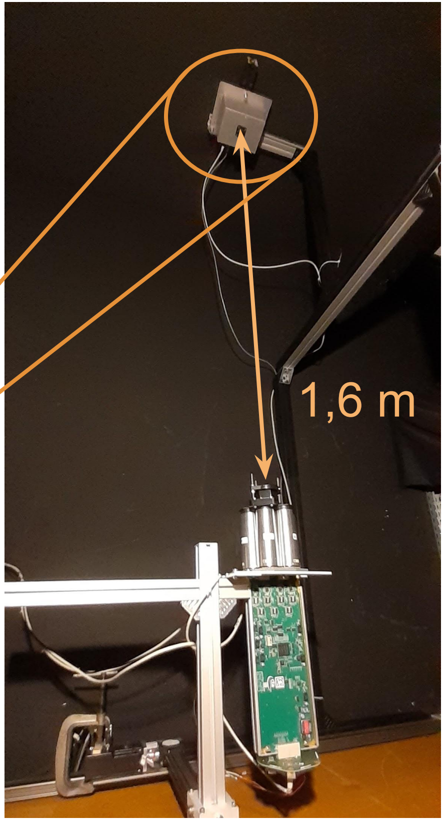

Part 2 - Simulation of CTAO-N site with MST/NectarCAM

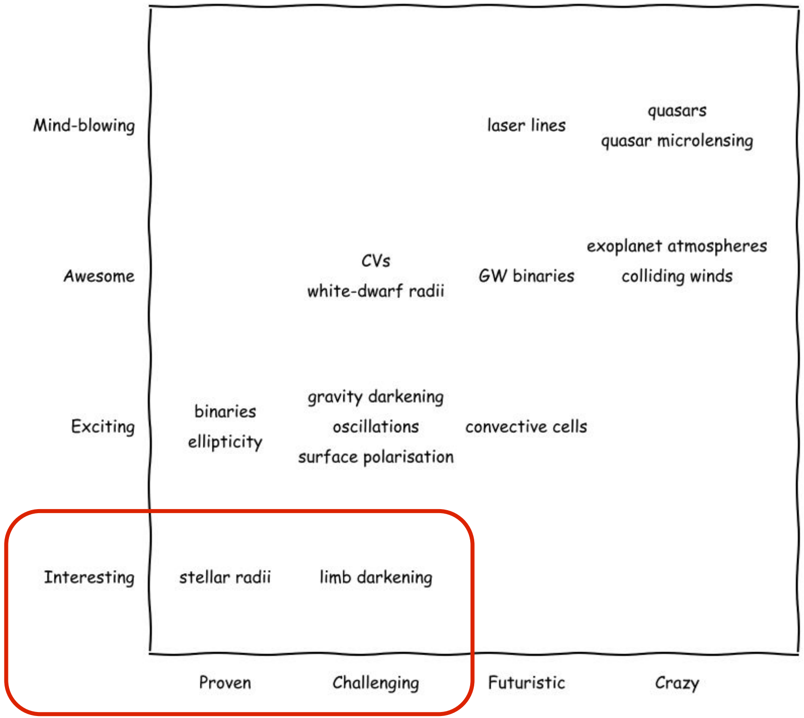

Credits: Prasenjit Saha

	Proven	Challenging	Futuristic	Crazy
Mind-blowing			laser lines	quasars quasar microlensing
Awesome		CVs white-dwarf radii	GW binaries	exoplanet atmospheres colliding winds
Exciting	binaries ellipticity	gravity darkening oscillations surface polarisation	convective cells	
Interesting	stellar radii	limb darkening		

Simulations of SII for CTAO-N

credits: Quentin Luce, Tarek Hassan, Jonathan Biteau

From the expected signal-to-noise ratio:

$$S/N = A \cdot \alpha(\lambda_0) \cdot q(\lambda_0) \cdot n(\lambda_0) \cdot |V|^2(\lambda_0, d) \cdot \sqrt{b_\nu} \cdot F^{-1} \cdot \sqrt{\frac{T}{2}} \cdot (1+\beta)^{-1} \cdot \sigma$$

with the visibility following a uniform disk model:

$$V(\lambda_0, d) = \left(2\frac{J_1(x)}{x}\right)^2 \qquad x = \frac{\pi b \theta}{\lambda}$$

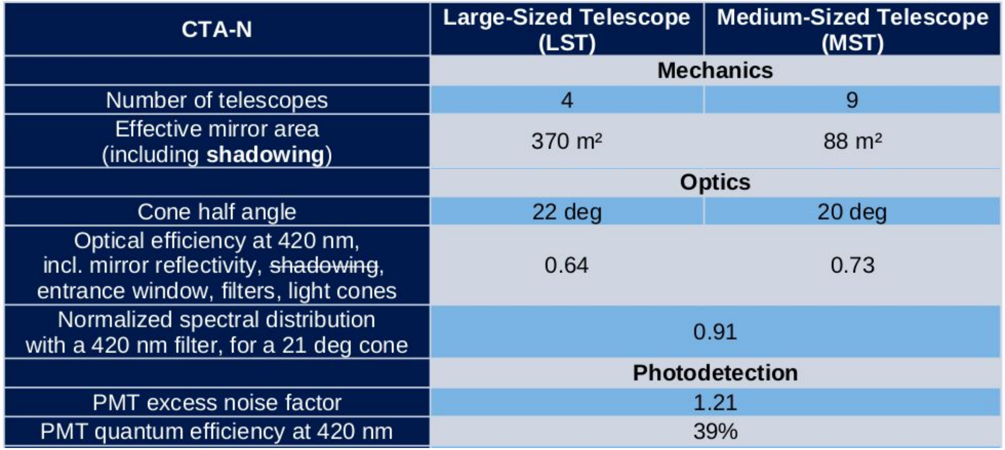

CTA-N	Large-Sized Telescope (LST)	Medium-Sized Telescope (MST)
	Mechanics	
Number of telescopes	4	9
Effective mirror area (including **shadowing**)	370 m²	88 m²
	Optics	
Cone half angle	22 deg	20 deg
Optical efficiency at 420 nm, incl. mirror reflectivity, ~~shadowing~~, entrance window, filters, light cones	0.64	0.73
Normalized spectral distribution with a 420 nm filter, for a 21 deg cone	0.91	
	Photodetection	
PMT excess noise factor	1.21	
PMT quantum efficiency at 420 nm	39%	

Observation time:
T ~ 2.5 h

Bandwidth:
500 MHz

Validation of simulation / analysis pipeline

credits: Quentin Luce, Tarek Hassan, Jonathan Biteau

~2h30 of observations, *θ* = 0.72 mas

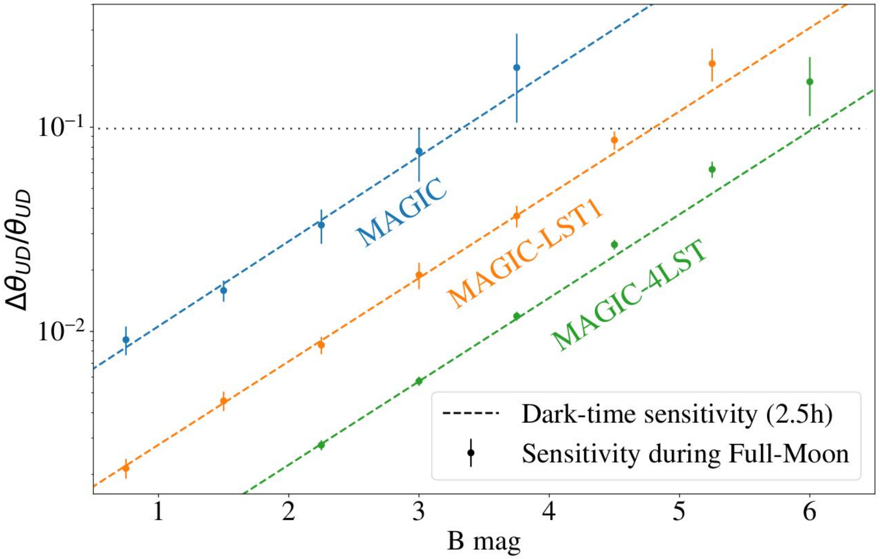

credits: Abe+ 2024 (MAGIC Collaboration)

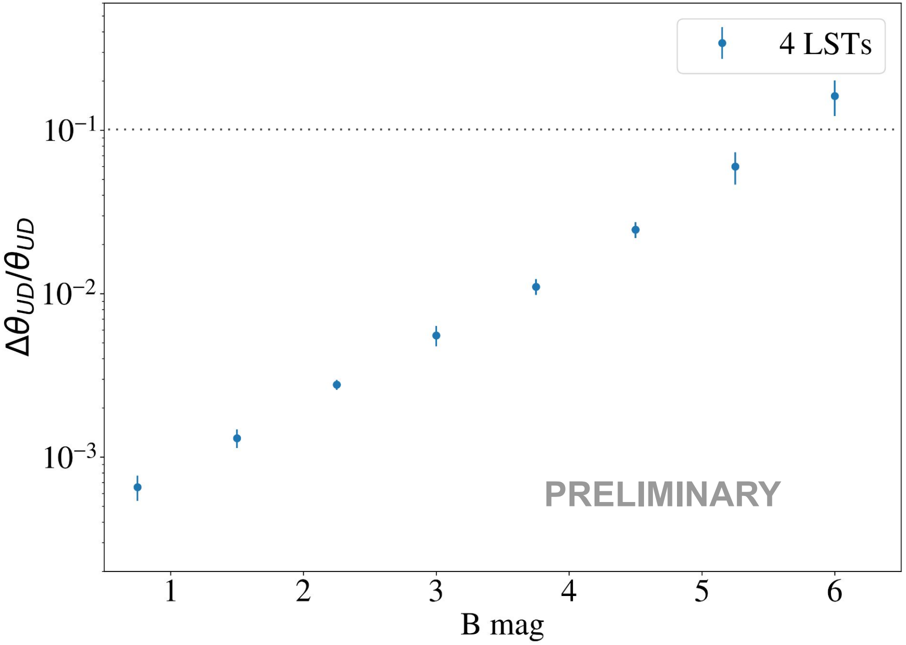

Simulations of SII for CTAO-N

credits: Quentin Luce, Tarek Hassan, Jonathan Biteau

From the expected signal-to-noise ratio:

$$S/N = A \cdot \alpha(\lambda_0) \cdot q(\lambda_0) \cdot n(\lambda_0) \cdot |V|^2(\lambda_0, d) \cdot \sqrt{b_\nu} \cdot F^{-1} \cdot \sqrt{\frac{T}{2}} \cdot (1+\beta)^{-1} \cdot \sigma$$

with the visibility following a uniform disk model:

$$V(\lambda_0, d) = \left(2\frac{J_1(x)}{x}\right)^2 \qquad x = \frac{\pi b \theta}{\lambda}$$

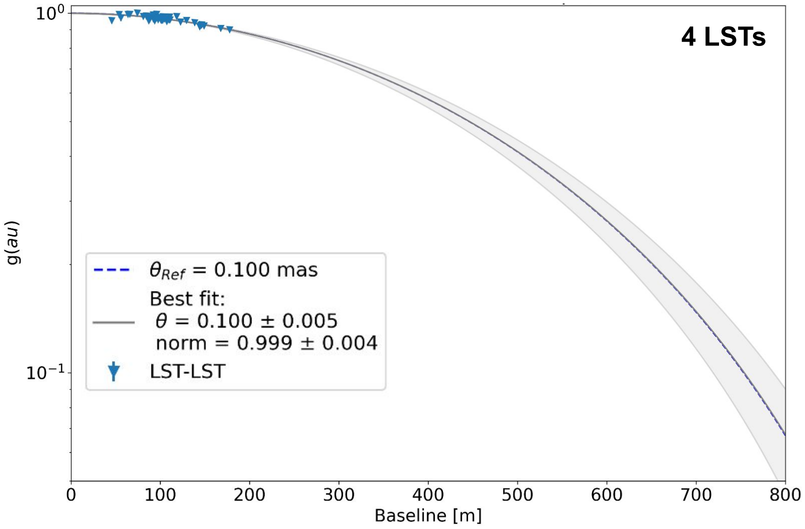

θ = 0.1 mas
B mag. = 3

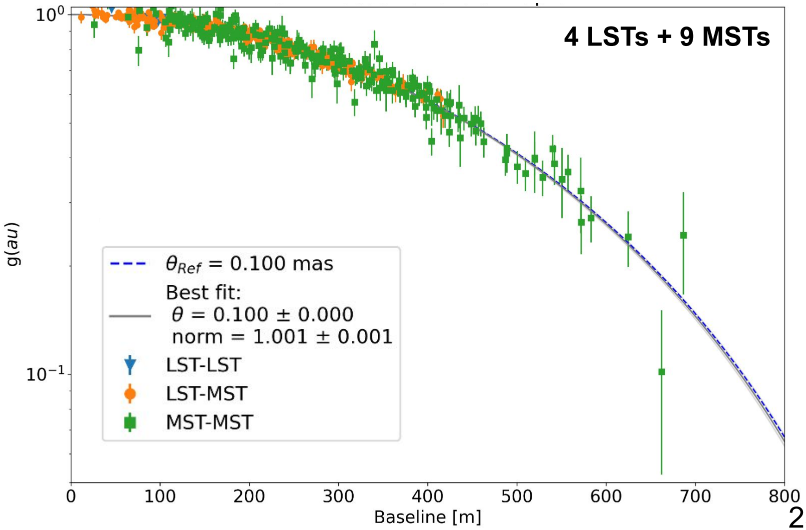

Simulations of SII for CTAO-N

credits: Quentin Luce, Tarek Hassan, Jonathan Biteau

From the expected signal-to-noise ratio:

$$S/N = A \cdot \alpha(\lambda_0) \cdot q(\lambda_0) \cdot n(\lambda_0) \cdot |V|^2(\lambda_0, d) \cdot \sqrt{b_\nu} \cdot F^{-1} \cdot \sqrt{\frac{T}{2}} \cdot (1+\beta)^{-1} \cdot \sigma$$

with the visibility following a uniform disk model:

$$V(\lambda_0, d) = \left(2\frac{J_1(x)}{x}\right)^2 \qquad x = \frac{\pi b \theta}{\lambda}$$

Precision on the measurement of the stellar radii?

Scan in B mag. from **0 to 6**,
and angular diameter $\boldsymbol{\theta}$ from **0.1 mas to 1.2 mas**

10 simulations per couple ($\boldsymbol{\theta}$, B mag.),

2 free parameters : normalization and $\boldsymbol{\theta}_{\mathrm{UD}}$

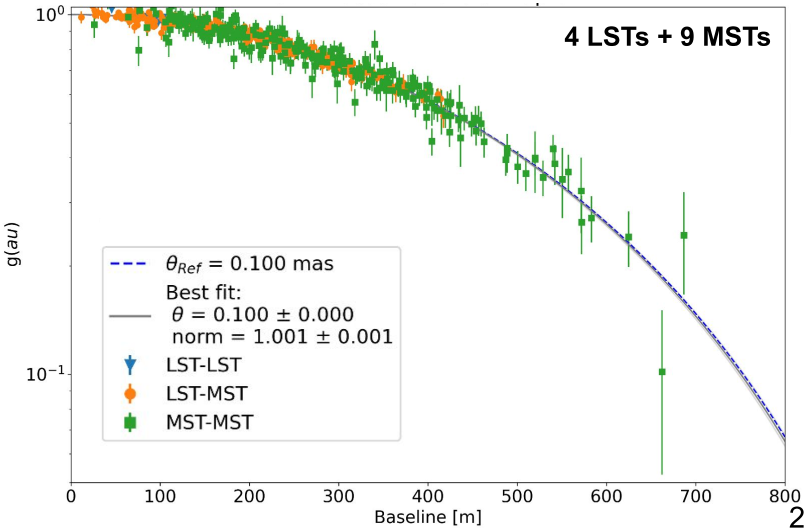

Resolution on the angular diameter - Uniform Disk model

credits: Quentin Luce, Tarek Hassan, Jonathan Biteau

~2h30 of observations

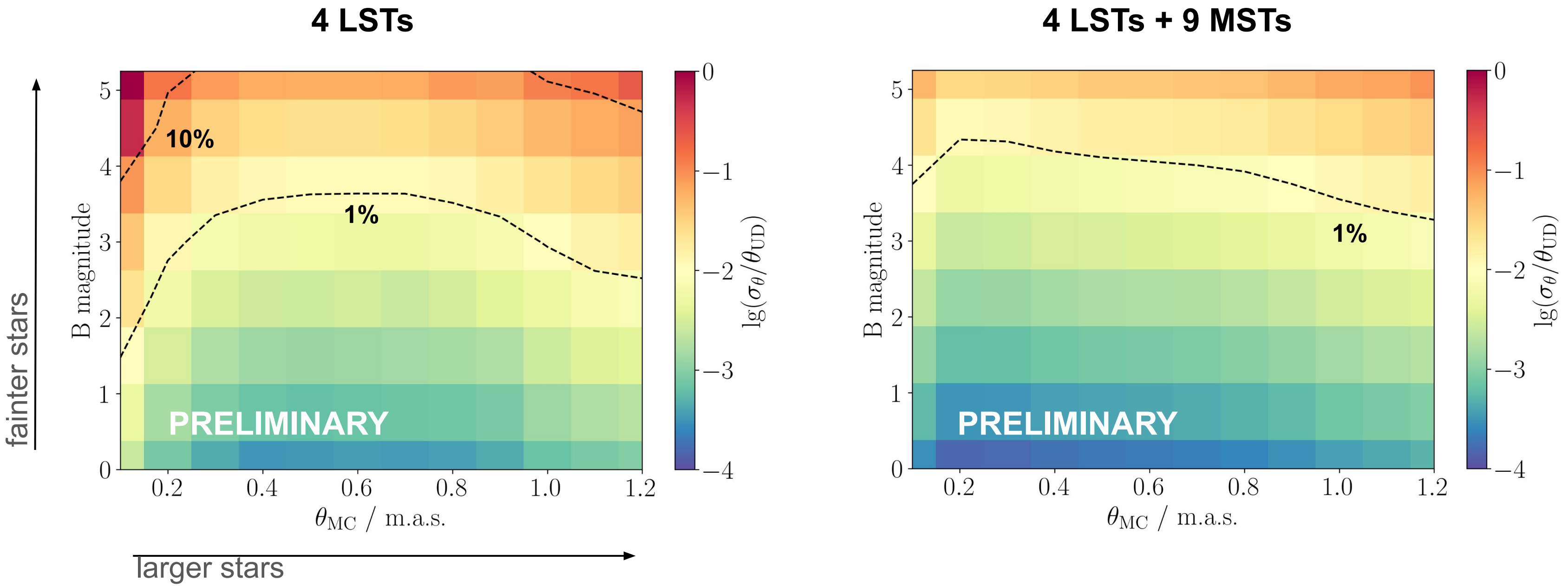

4 LSTs

4 LSTs + 9 MSTs

→ **4 LSTs:** **~ 1% precision on θ_{UD}** for stars with B mag. < 3

→ **4 LSTs + 9 MSTs:** **~ 1% precision on θ_{UD}** for stars with B mag. < 4

Target stars

credits: Lucijana Stanic
Adapted from https://target-stars-sii.streamlit.app

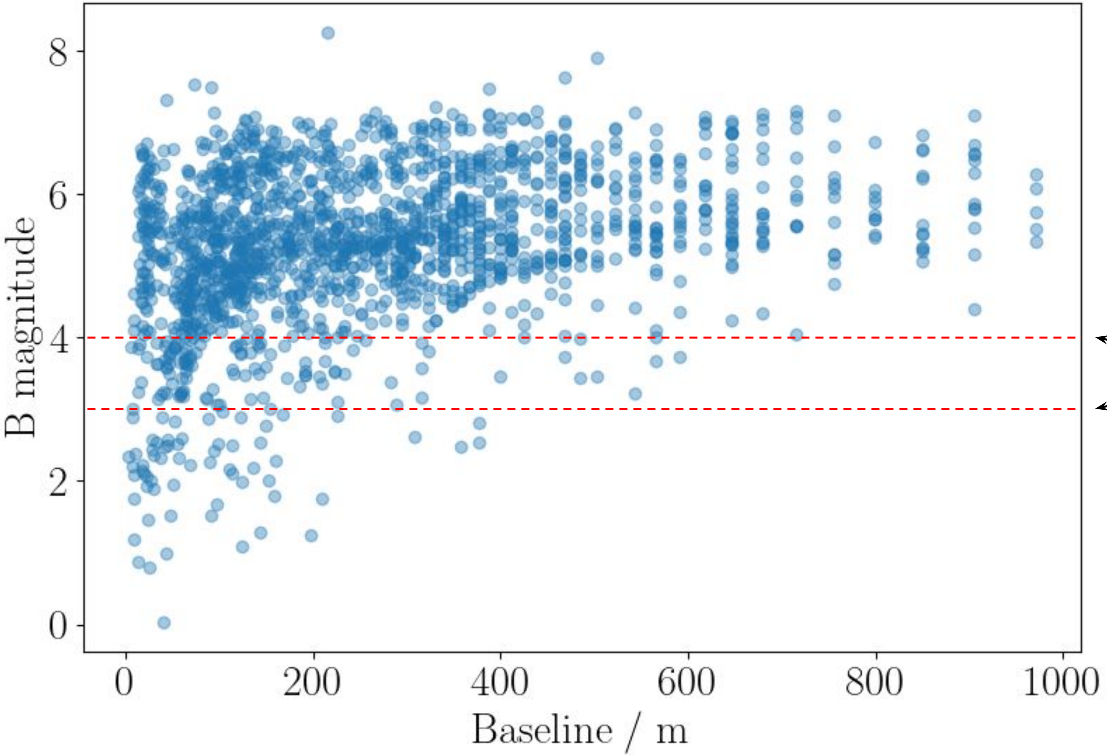

Number of stellar radii **reconstructed with a precision of 1%** in the Northern hemisphere

4 LSTs + 9 MSTs: **~170 stars**
4 LSTs: **~60 stars**
for T ~2h30

Looking at limb-darkening

credits: Quentin Luce, Tarek Hassan, Jonathan Biteau

Linear Limb-Darkened Model $\frac{I(\lambda,\mu=\cos\psi)}{I_0} = 1 - u_\lambda(1-\mu)$

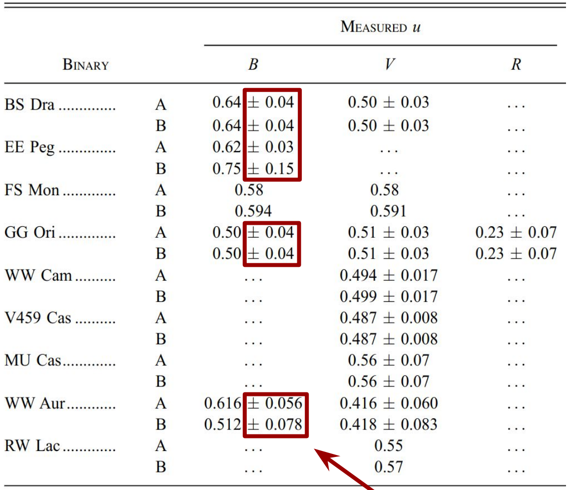

BINARY		MEASURED u		
		B	V	R
BS Dra	A	0.64 ± 0.04	0.50 ± 0.03	. . .
	B	0.64 ± 0.04	0.50 ± 0.03	. . .
EE Peg	A	0.62 ± 0.03	. . .	. . .
	B	0.75 ± 0.15	. . .	. . .
FS Mon	A	0.58	0.58	. . .
	B	0.594	0.591	. . .
GG Ori	A	0.50 ± 0.04	0.51 ± 0.03	0.23 ± 0.07
	B	0.50 ± 0.04	0.51 ± 0.03	0.23 ± 0.07
WW Cam	A	. . .	0.494 ± 0.017	. . .
	B	. . .	0.499 ± 0.017	. . .
V459 Cas	A	. . .	0.487 ± 0.008	. . .
	B	. . .	0.487 ± 0.008	. . .
MU Cas............	A	. . .	0.56 ± 0.07	. . .
	B	. . .	0.56 ± 0.07	. . .
WW Aur...........	A	0.616 ± 0.056	0.416 ± 0.060	. . .
	B	0.512 ± 0.078	0.418 ± 0.083	. . .
RW Lac	A	. . .	0.55	. . .
	B	. . .	0.57	. . .

Credits: D. Heyrovsy, ApJ 2007

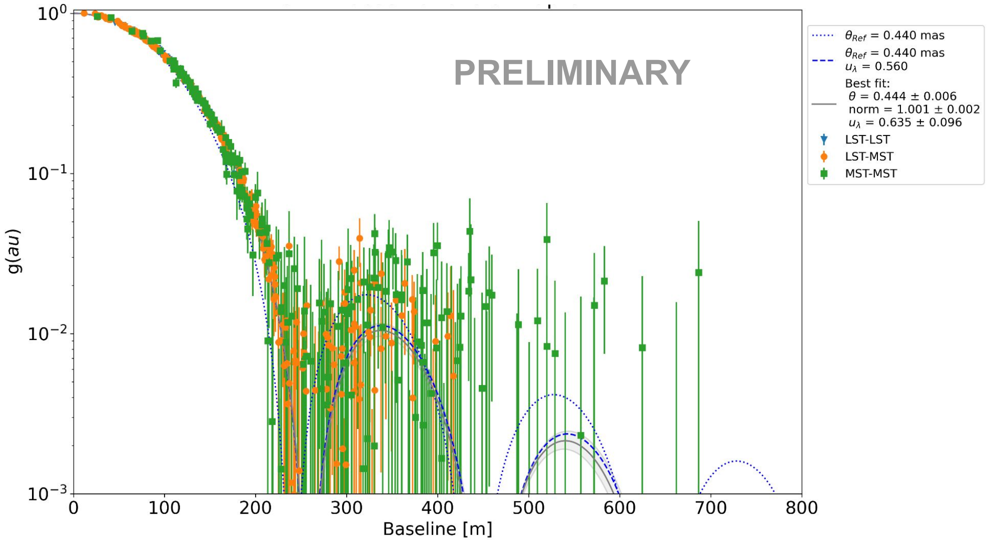

10% precision w/ eclipsing binaries

Note: Constraints useful for studies of exoplanet transit?

Looking at limb-darkening

credits: Quentin Luce, Tarek Hassan, Jonathan Biteau

From the expected signal-to-noise ratio:

$$S/N = A \cdot \alpha(\lambda_0) \cdot q(\lambda_0) \cdot n(\lambda_0) \cdot |V|^2(\lambda_0, d) \cdot \sqrt{b_\nu} \cdot F^{-1} \cdot \sqrt{\frac{T}{2}} \cdot (1+\beta)^{-1} \cdot \sigma$$

with the visibility including limb-darkening effect:

$$V(\lambda_0, d) = \left(\frac{1-u_\lambda}{2} + \frac{u_\lambda}{3}\right)^{-2} \left[(1-u_\lambda)\frac{J_1(x)}{x} + u_\lambda \sqrt{\frac{\pi}{2}} \frac{J_{3/2}(x)}{x^{3/2}}\right]^2$$

$$\frac{I(\lambda, \mu = \cos\psi)}{I_0} = 1 - u_\lambda(1-\mu)$$

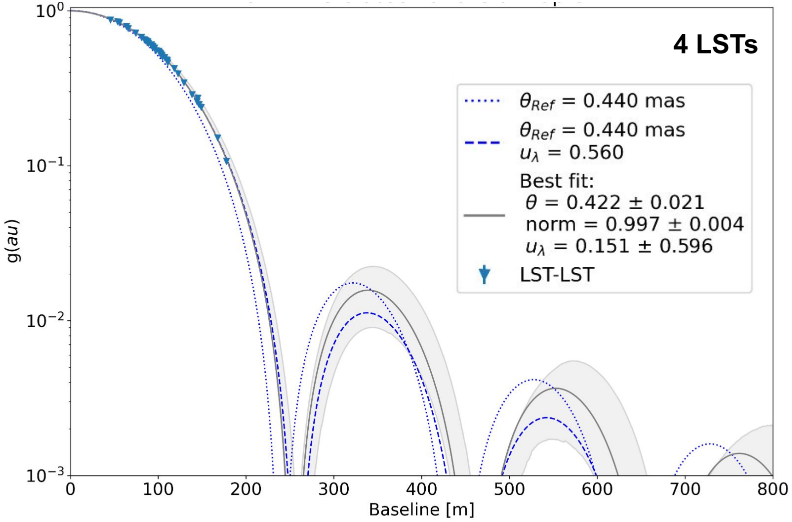

***κ* Ori**

***θ* = 0.44 mas**

B mag. = 1.88

u_λ = 0.56

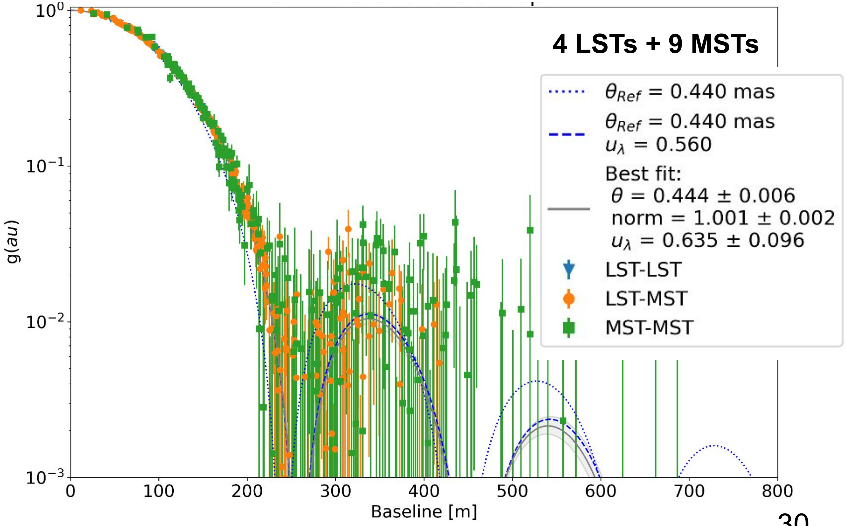

Looking at limb-darkening

credits: Quentin Luce, Tarek Hassan, Jonathan Biteau

From the expected signal-to-noise ratio:

$$S/N = A \cdot \alpha(\lambda_0) \cdot q(\lambda_0) \cdot n(\lambda_0) \cdot |V|^2(\lambda_0, d) \cdot \sqrt{b_\nu} \cdot F^{-1} \cdot \sqrt{\frac{T}{2}} \cdot (1+\beta)^{-1} \cdot \sigma$$

with the visibility including limb-darkening effect:

$$V(\lambda_0, d) = \left(\frac{1-u_\lambda}{2} + \frac{u_\lambda}{3}\right)^{-2} \left[(1-u_\lambda)\frac{J_1(x)}{x} + u_\lambda \sqrt{\frac{\pi}{2}} \frac{J_{3/2}(x)}{x^{3/2}}\right]^2$$

$$\frac{I(\lambda, \mu = \cos\psi)}{I_0} = 1 - u_\lambda(1-\mu)$$

Precision on the measurement of the stellar radii?

Scan in B mag. from **0 to 6**,
and angular diameter $\boldsymbol{\theta}$ from **0.1 mas to 1.2 mas**

10 simulations per couple ($\boldsymbol{\theta}$, B mag.)

2 reconstructions:

- Uniform Disk fit:
  2 free parameters = normalization and $\boldsymbol{\theta}_{\mathrm{UD}}$
- Limb-Darkening fit:
  3 free parameters = normalization, $\boldsymbol{\theta}_{\mathrm{LD}}$ and $\boldsymbol{u_\lambda}$

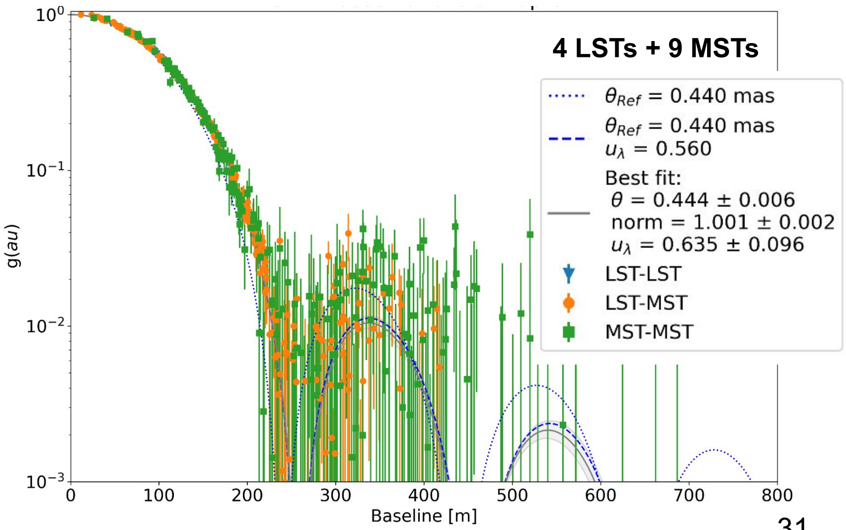

Resolution on the angular diameter: Uniform Disk fit

credits: Quentin Luce, Tarek Hassan, Jonathan Biteau

~2h30 of observations, u_λ= 0.4:

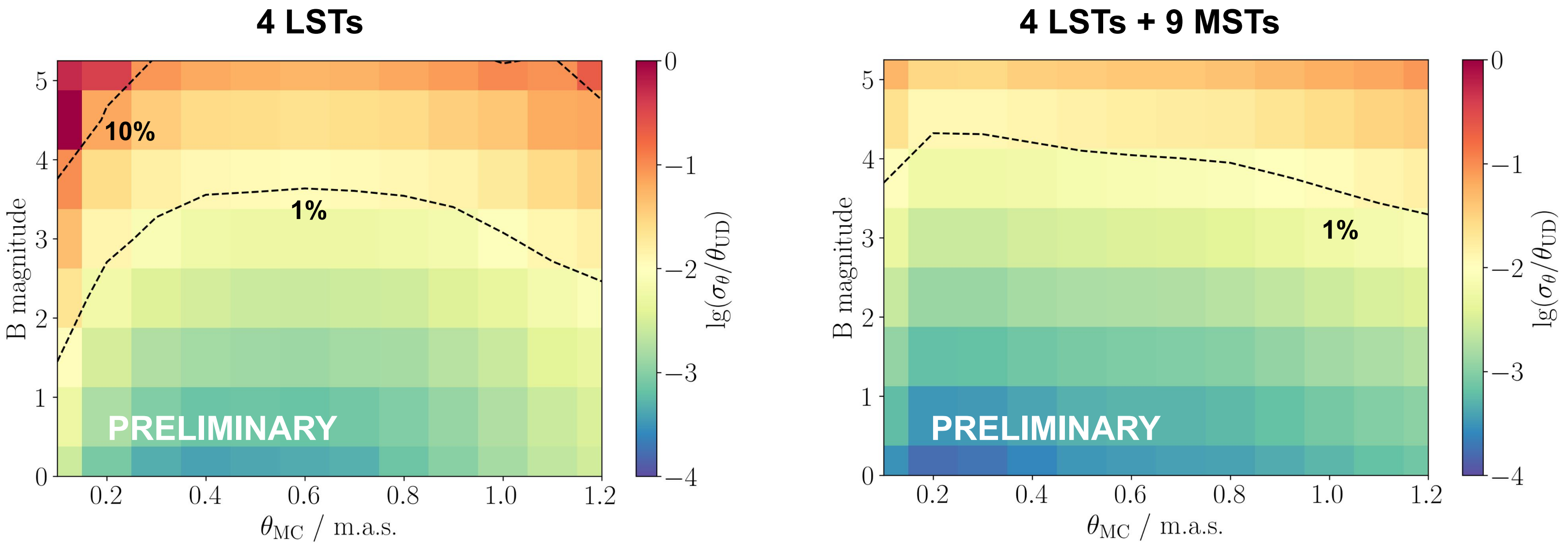

→ **4 LSTs:** **~ 1% precision on θ_{UD}** for stars with B mag. < 3

→ **4 LSTs + 9 MSTs:** **~ 1% precision on θ_{UD}** for stars with B mag. < 4

But careful about the bias!

Resolution on the angular diameter: Limb-Darkening fit

credits: Quentin Luce, Tarek Hassan, Jonathan Biteau

~2h30 of observations, u_λ= 0.4:

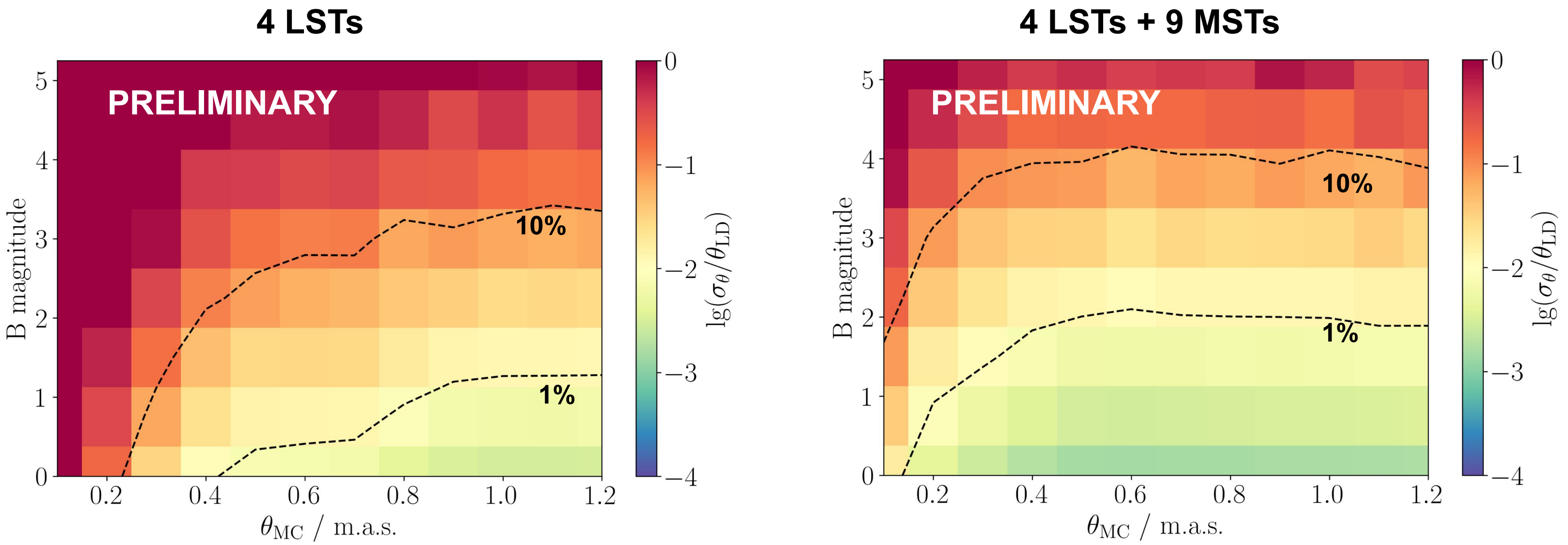

→ **4 LSTs:** **~ 1% precision on θ_{LD}** for stars with B mag. < 1 and large radii (***θ*** > 0.7 mas)

→ **4 LSTs + 9 MSTs:** **~ 1% precision on θ_{LD}** for stars with B mag. < 2 (***θ*** > 0.2 mas)

Bias on the angular diameter

credits: Quentin Luce, Tarek Hassan, Jonathan Biteau

~2h30 of observations, B magnitude = 1.5, 4 LSTs + 9 MSTs:

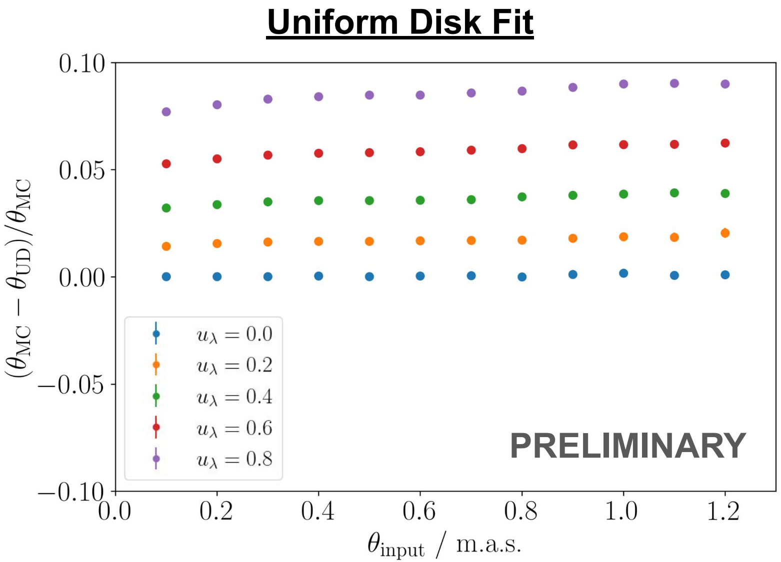
Uniform Disk Fit

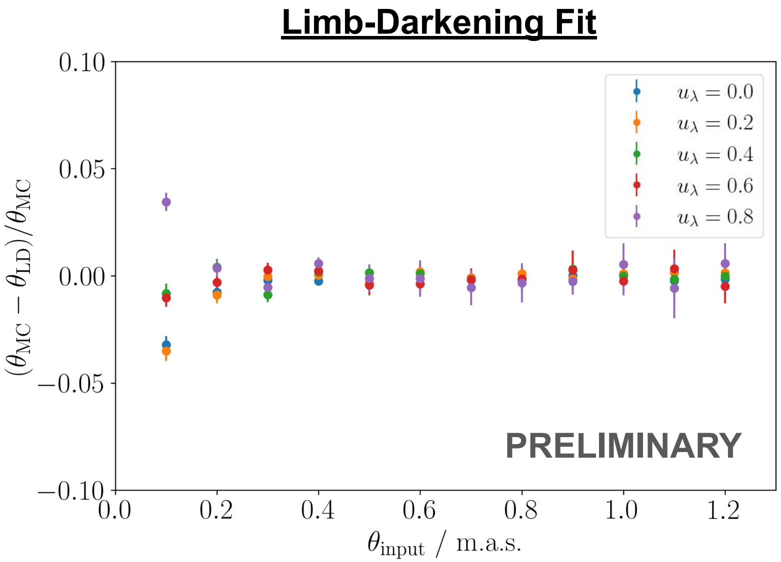
Limb-Darkening Fit

→ **Uniform Disk fit:** **~ 1% precision on θ_{UD}** but with a bias evolving with u_λ

→ **Limb-Darkening fit:** **~ 1% precision on θ_{LD}** for stars with B mag. < 2, unbiased if θ > 0.2 mas

Constraining u_λ?

~2h30 of observations, u_λ= 0.4:

Linear Limb-Darkened Model: $\frac{I(\lambda, \mu=\cos\psi)}{I_0} = 1 - u_\lambda(1-\mu)$

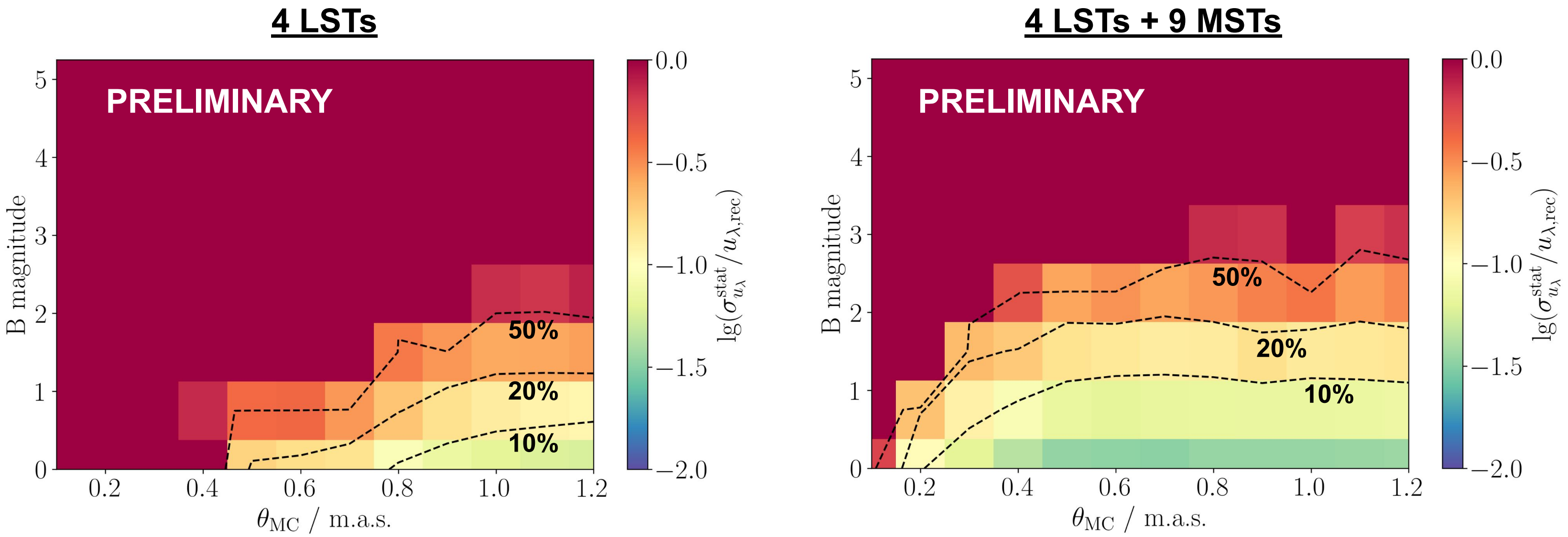

→ **4 LSTs:** **~ 10% precision on θ_{LD}** for stars with B mag. < 0.5 and large radii (***θ*** > 0.8 mas)

→ **4 LSTs + 9 MSTs:** **~ 10% precision on θ_{LD}** for stars with B mag. < 1.2 (***θ*** > 0.2 mas)

Target stars

credits: Lucijana Stanic
Adapted from https://target-stars-sii.streamlit.app

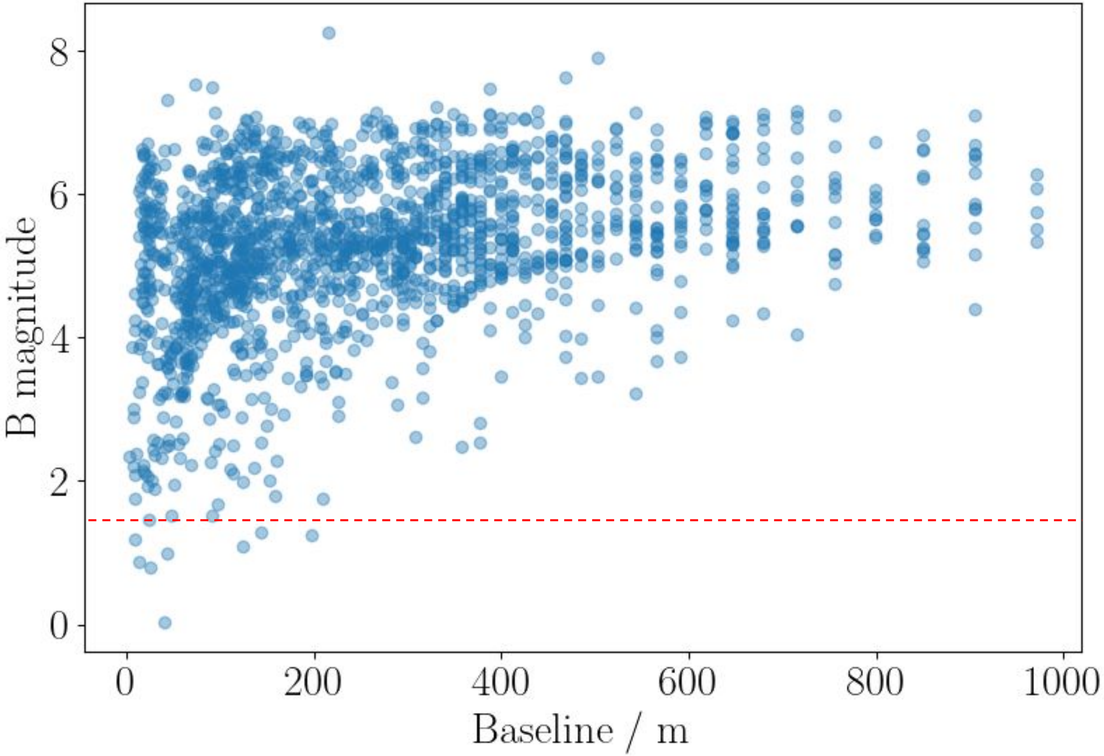

Number of stars **with 10% precision on limb-darkening coefficient** in the Northern hemisphere (B mag. < 1.2)

4 LSTs + 9 MSTs: **~10 stars**
(examples: αLyr, εCMa) **for T ~2h30**

Summary and next steps

credits: Quentin Luce, Tarek Hassan, Jonathan Biteau

Significant increase of the science reach with 4 LSTs + 9 MSTs with respect to 4 LSTs

- triple the number of high-precision (sub-percent) measurement of stellar radii
- opens the possibility for precision (<10%) measurement of limb-darkening

Investigation limited to Prasenjit's "interesting" science cases (i.e. below "exciting" level)

- further exploration of science case and CTAO-S alpha-configuration surely promising!

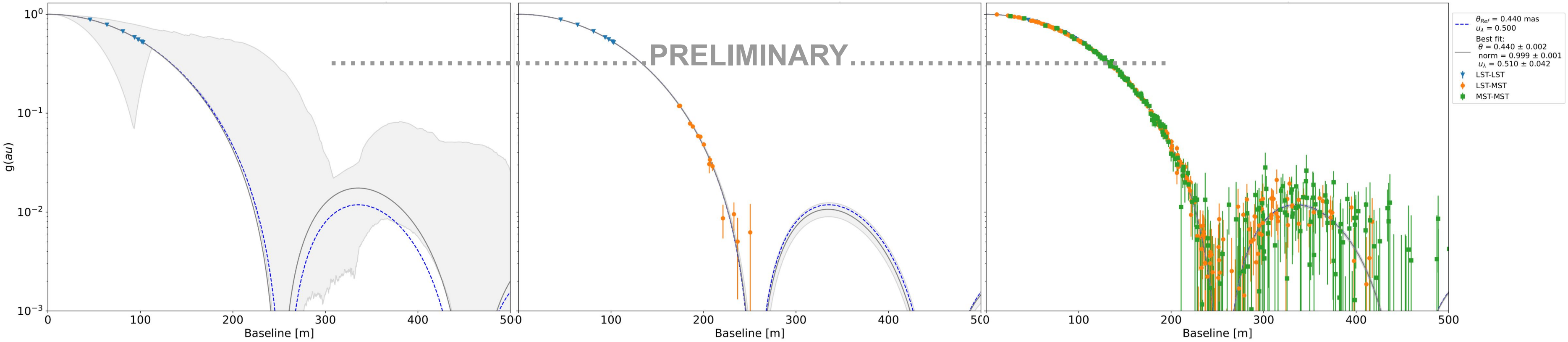

1st and 2nd LSTs | **1st and 2nd LSTs + 1st MST** | **4 LSTs + 9 MSTs**

Next year → **Next-to-next year** → **Next PhD cycle**

Backup

Stellar intensity interferometry (SII): concept

Initiated by Hanbury-Brown & Twiss

Development of the Narrabri Stellar Intensity Interferometer

Distance *d* = 10-200m between the two telescopes (6.5m diameter)

Single PMT with 20% Q.E. at $\lambda = 440$ nm on each telescope, $I_{anode} \sim 100\ \mu A$

Measurement of the angular diameter of 32 stars

Time correlation of 2 PMTs ↔ constructive interference of 2 photons pathways

→ angular extent of an incoherent light source with
$\Delta\theta = \lambda / d \sim 80\ \mu as \times (\lambda / 400\ nm) \times (d / 1\ km)^{-1}$

Revived by current generation IACT, with vast science case

Stellar diameters, winds, photosphere; Binary systems, accretion disks; Novae and other transient events; Rapid rotators; Exoplanet imaging; Stellar occultation: trans-Neptunian / Kuiper-belt objects (see SII2023 workshop)

Observations during moon time: increase of IACT duty cycle!

Narrabri 6.5m tels (1963-1974)

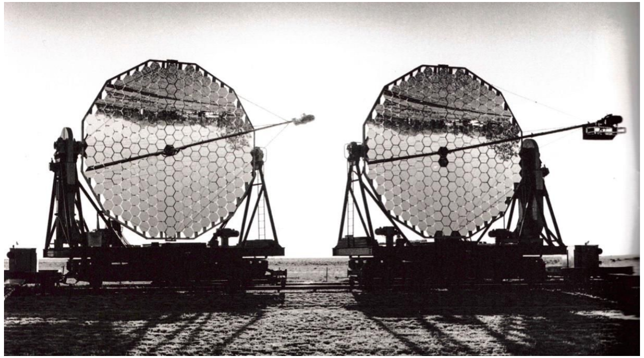

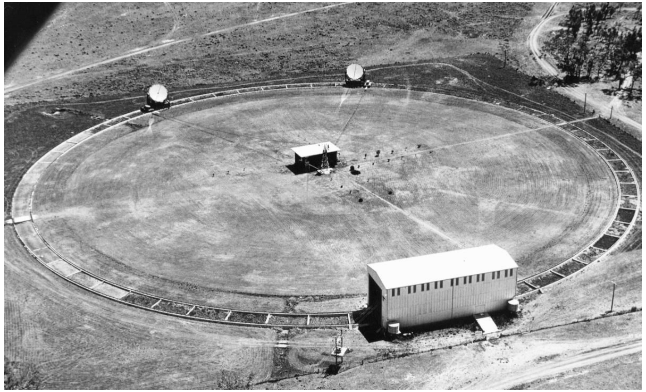

Uniform disk model: performance

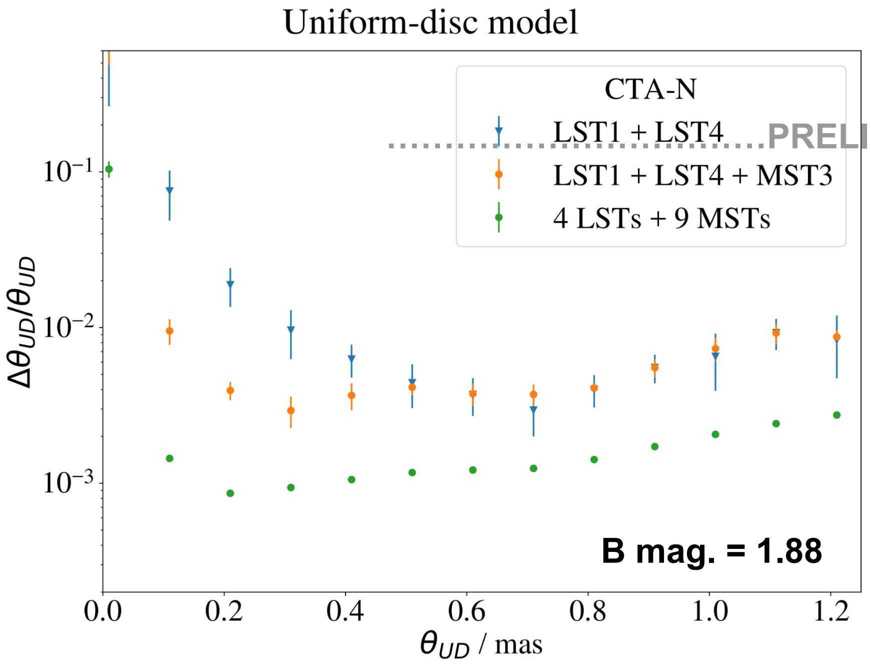
Uniform-disc model

B mag. = 1.88

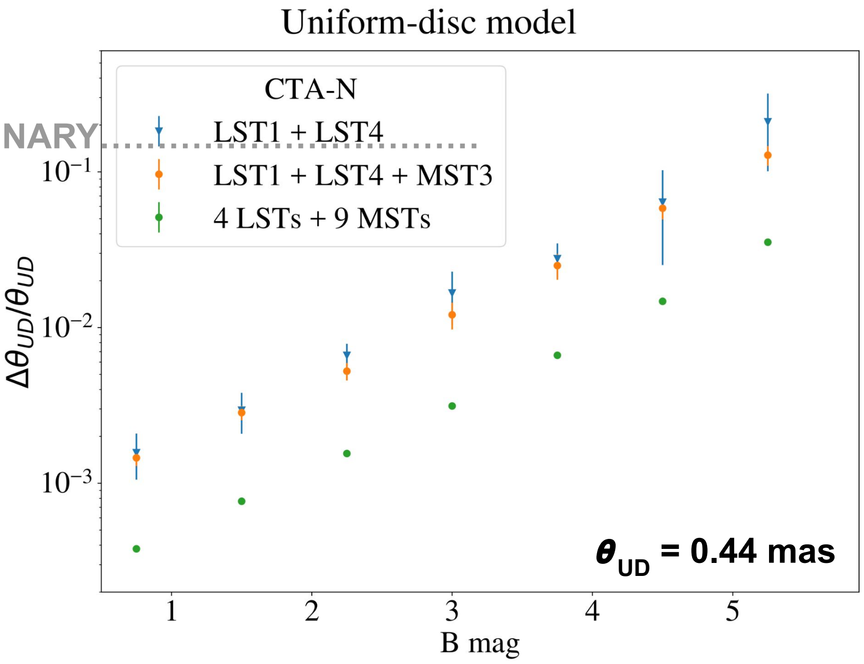
Uniform-disc model

θ_{UD} = 0.44 mas

Limb darkened model: performance

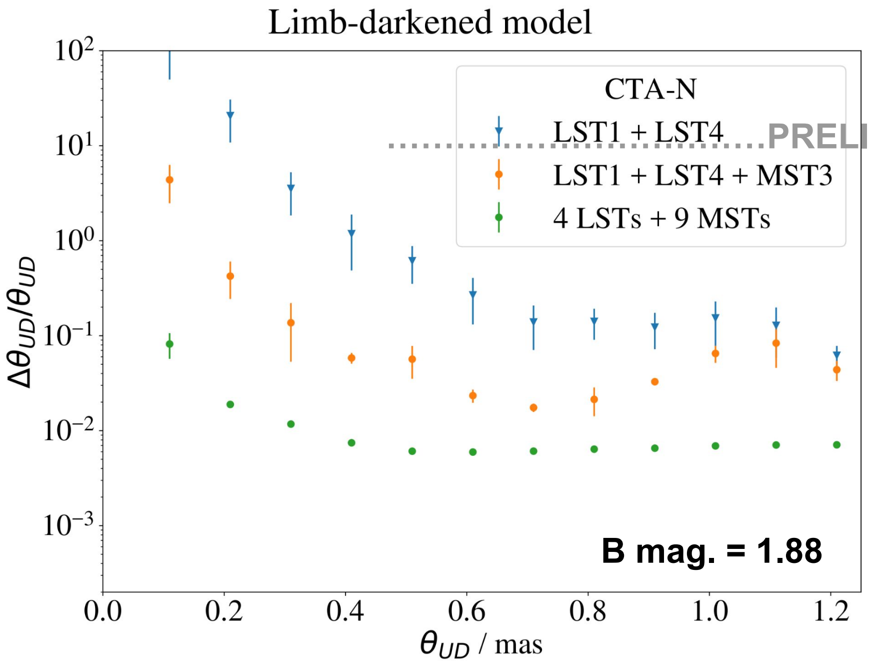

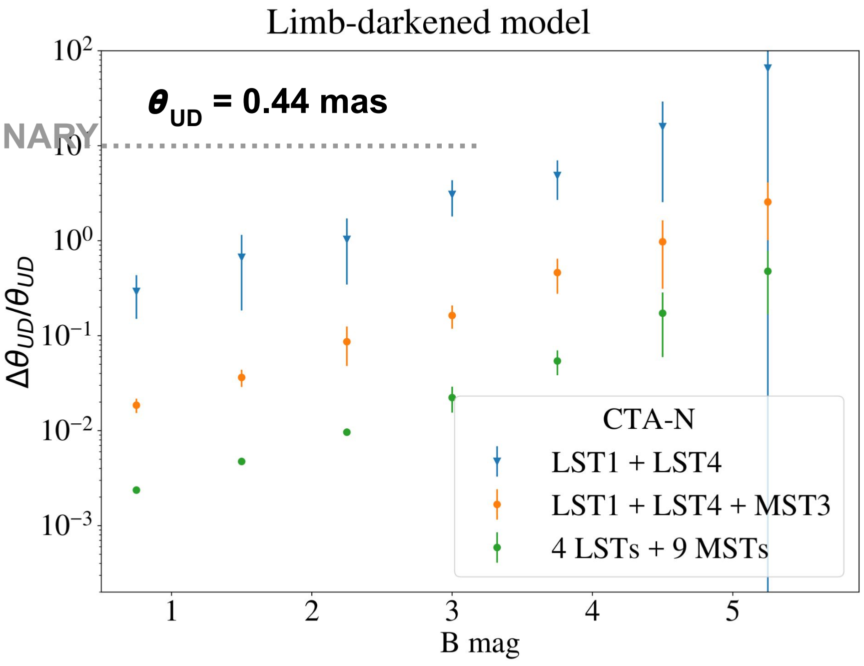

Constraining u_λ? 4 LSTs

$$\frac{I(\lambda,\mu{=}\cos\psi)}{I_0} = 1 - u_\lambda(1-\mu)$$

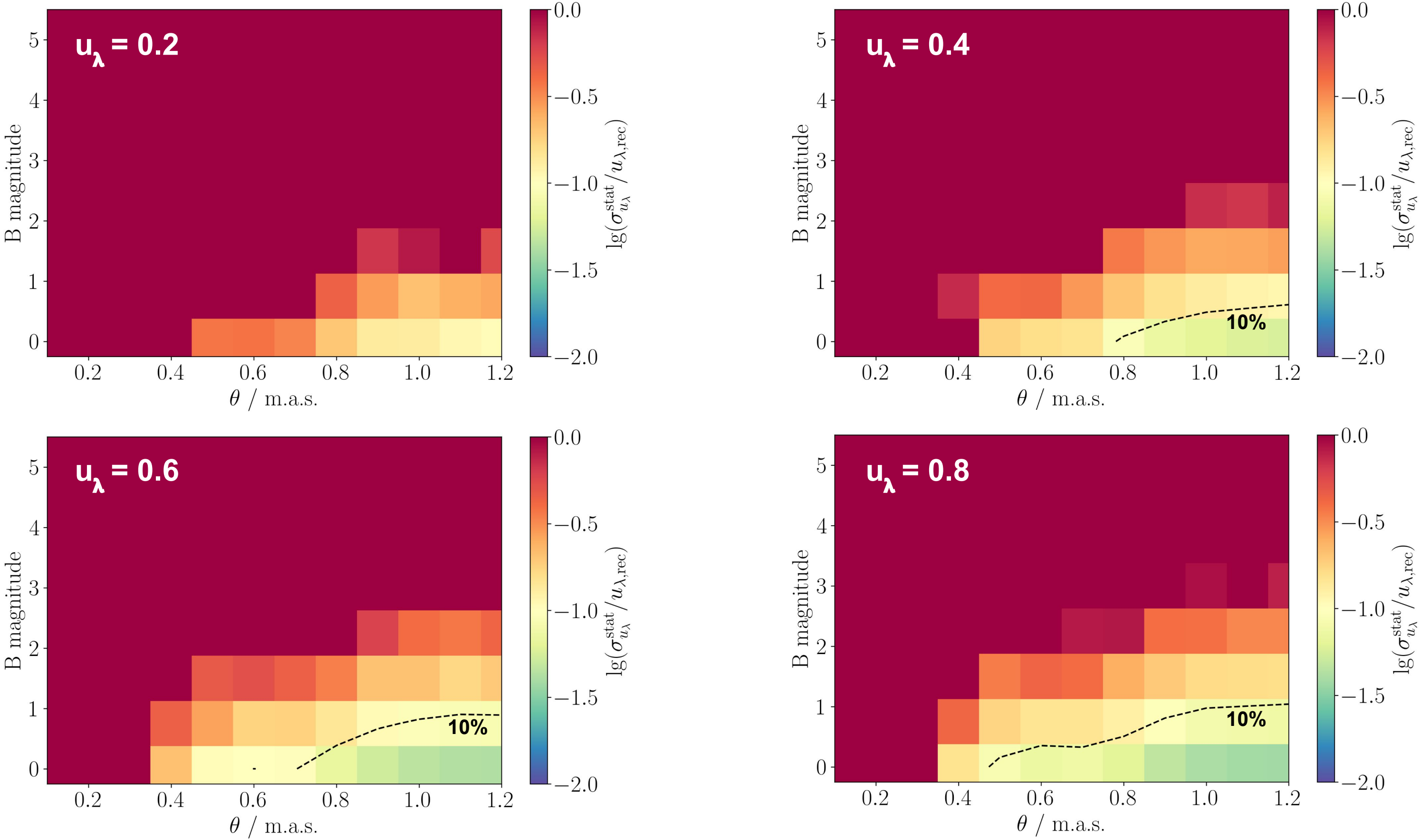

Constraining u_λ? 4 LSTs + 9 MSTs

$$\frac{I(\lambda,\mu=\cos\psi)}{I_0} = 1 - u_\lambda(1-\mu)$$